International Journal of Minerals, Metallurgy and Materials
Volume 30, Number 10, October 2023, Page 1933
https://doi.org/10.1007/s12613-023-2694-6

Invited Review

Recent advances and influencing parameters in developing electrode materials for symmetrical solid oxide fuel cells

Wan Nor Anasuhah Wan Yusoff[1)], *Nurul Akidah Baharuddin*[1),✉], *Mahendra Rao Somalu*[1)], *Andanastuti Muchtar*[1,2)], *Nigel P. Brandon*[3)], *and Huiqing Fan*[4)]

1) Solid Oxide Fuel Cell Group, Fuel Cell Institute, Universiti Kebangsaan Malaysia, 43600, UKM Bangi, Selangor, Malaysia
2) Department of Mechanical and Manufacturing Engineering, Faculty of Engineering and Built Environment, Universiti Kebangsaan Malaysia, 43600, UKM Bangi, Selangor, Malaysia
3) Faculty of Engineering, 2.06 Faculty Building, Imperial College London, SW7 2 AZ, UK
4) State Key Laboratory of Solidification Processing, School of Materials Science and Engineering, Northwestern Polytechnical University, Xi'an 710072, China
(Received: 19 April 2023; revised: 19 June 2023; accepted: 21 June 2023)

Abstract: This article delivers a robust overview of potential electrode materials for use in symmetrical solid oxide fuel cells (S-SOFCs), a relatively new SOFC technology. To this end, this article provides a comprehensive review of recent advances and progress in electrode materials for S-SOFC, discussing both the selection of materials and the challenges that come with making that choice. This article discussed the relevant factors involved in developing electrodes with nano/microstructure. Nanocomposites, e.g., non-cobalt and lithiated materials, are only a few of the electrode types now being researched. Furthermore, the phase structure and microstructure of the produced materials are heavily influenced by the synthesis procedure. Insights into the possibilities and difficulties of the material are discussed. To achieve the desired microstructural features, this article focuses on a synthesis technique that is either the most recent or a better iteration of an existing process. The portion of this analysis that addresses the risks associated with manufacturing and the challenges posed by materials when fabricating S-SOFCs is the most critical. This article also provides important and useful recommendations for the strategic design of electrode materials researchers.

Keywords: nano composites; electrode; microstructure tailoring; oxidation; symmetrical solid oxide fuel cell

1. Introduction

The world is facing a challenge in finding applicable, sustainable, and clean replacements for fossil fuels [1–3]. Fossil fuel implementation has led to tremendous environmental, political, and economic issues [4–6]. Energy storage systems have particular, strict operational requirements such as operating duration, dynamic requirements, and power-to-energy ratios [7–9]. Renewable energy is certainly the most highlighted research topic in recent years because it can deliver over 80% of energy generation in four decades globally [10–12]. Current progress in this field includes the conversion of electrical energy produced from renewable sources into other forms of zero-carbon energy carriers, such as hydrogen [13]. This approach allows renewable energy to be transported easily to other locations and then coupled with fuel cells to convert the hydrogen back into electrical power.

Various fuel cell types are available, including direct methanol, proton-exchange membrane, phosphoric acid, molten carbonate, alkaline, microbial, and solid oxide fuel cells (SOFCs), differing in terms of the electrolyte type and the operating temperature [14–16]. Among the fuel cell types, SOFC is currently regarded as the promising energy conversion technology compared with biogas-fueled or natural gas-fueled combustion engines because it offers a remarkable advantage in terms of efficiency and fuel flexibility [17–19], together with low emissions of NO_x relative to combustion engines [20–21]. Furthermore, given their high operating temperature (600–1000°C), high-quality heat waste is produced with the potential for reformation and direct electrochemical oxidation of hydrocarbon fuels [22]. SOFC developments have been studied for use in fuel cell–gas turbine hybrids, cogeneration/trigeneration, and industrial applications [23].

The durability of SOFCs is relatively challenging because they operate at high temperatures [24]. Thus, the recent trend in SOFC development focuses on lowering the operating temperature to improve the lifetime [25]. A conventional SOFC stack are composed of a cathode (air electrode), an electrolyte, and an anode (fuel electrode) [26], where the state-of-the-art electrode materials are composite materials to ensure a low thermal expansion difference. Potential cathode material should have sufficient porosity to ensure optimum oxygen transportation toward the reaction site. The catalytic

✉ Corresponding author: Nurul Akidah Baharuddin E-mail: akidah@ukm.edu.my

property of the cathode also plays a crucial role in the oxygen reduction reaction (ORR) that determines the charge transfer rate and lowers the activation energy needed to start the operation, especially at low operating temperatures. The thermal expansion coefficient (TEC) should be matched as closely as possible to the electrolyte material to ensure a stable mechanical aspect. During the operation, the chemical compatibility of the material should be considered to prevent any undesired reaction between the neighboring components fabricated because this situation may degrade cell stability and durability.

The anode component, known as the fuel electrode, is another electrode fixed on the opposite side of the cathode material on the electrolyte side. O^{2-} ions are produced on the cathode side and transferred to the anode side via the dense, ionically conducting electrolyte material. The release of electrons because of oxidation completes the external circuit, thereby leading to electric current formation [27]. Conventional nickel-based anodes exhibit two major roles, as a catalyst in methane reforming and at the site for electrochemical oxidation [28]. For an active area with sufficient porosity, a triple phase boundary (TPB) promotes electrical conduction and excellent catalytic activity [29–30]. A dense electrolyte material enables ionic conduction to this active interface.

The electrolyte component commonly appears with physical properties similar to ceramics with high density and low porosity. This component is fabricated between the air electrode and the fuel electrode. The electrolyte material has an important role because it provides a path of ionic conduction from the anode to the cathode side [31]. Yttria-stabilized zirconia (YSZ) is an example of an electrolyte commonly used in SOFC applications because YSZ exhibits good performance and meets most of the requirements as an electrolyte candidate for SOFC application. The electrolyte has the following listed characteristics: (1) high density and ionic conductivity (0.01–0.1 S/cm for 1–100-mm thickness); (2) chemical, phase, and morphological stability in reducing and oxidizing environments; (3) low electronic conductivity — high electronic conductivity results in voltage and unwanted fuel consumption loss through internal short-circuiting currents; (4) high thermal stability of materials; (5) sufficient mechanical strength.

SOFC application for practical use is still obstructed by component flaws, including the catalytic performance of the cathode and carbon or sulfur deposition at the anode [32]. A conventional SOFC device incorporates three main components: electrode (cathode and anode) and electrolyte. All these components are mostly made of ceramic-based materials with distinct configurations [33]. Diversification of components requires considerable work, especially during fabrication, in addition to the accompanying efforts, time, and cost [34]. Another issue is the possibility of incompetent reactivity between the components due to a slight glitch or a fault during fabrication [35].

Moreover, an excellent performance of the SOFC system at lower operational temperature can be accomplished by two methods: first, by enhancing the existing materials with greater conductivity, for instance, electrolyte thickness, and second, by optimizing various configurations such as symmetrical SOFCs (S-SOFCs) that can reduce the production and running costs [36]. The possibility of using the same materials for SOFC electrodes, known as S-SOFCs, may reduce manufacturing and operating costs [37]. Additionally, it requires easy and quick cell assembly and the potential to recycle cells by reversing the gas flow to eliminate probable carbon contamination or sulfur toxicity by using hydrocarbons or biogas as fuels [38]. However, the idea of using the same substrate on all SOFC electrodes as symmetrical setups has several drawbacks. Currently, one of the main gaps in the development of S-SOFCs is to determine the electrode material candidates that possess excellent electrical conductivity, catalytic activity, and chemical stability, as well as oxidation and reduction properties [39].

The fundamental SOFC parts (electrolyte, cathode, anode, and interconnect) have been studied by Ruiz-Morales [40] in his 2011 study of S-SOFC and reversible SOFC (R-SOFC) materials. Single-phase and stable-phase materials, composite electrodes, and reducible electrodes were all the focus of Su *et al.* [41] in 2015. Thus, the most up-to-date developments in electrode technology for S-SOFC and a selection of a few for reversible SOFC (R-SOFC) were analyzed. The advanced synthesis process is addressed, along with its benefits and limitations, with a focus on the preliminary selection of the basis nano/micro-structured materials. This analysis comprises five main parts. Section 1 provides an overview of the world's energy needs before moving on to detail the benefits of fuel cells, the SOFC idea, and the lingering limits of this technology. Section 2 presents a summary of the classes of materials that might serve as S-SOFC electrode candidates from various backgrounds. Next, Section 3 provides an in-depth analysis of the elements that have guided the ongoing research on S-SOFC electrode materials, with an emphasis on the pros and cons of common synthesis procedures. In the next section, the material enhancement method is also discussed prior to the common fabrication risks of the SOFC single cell. The typical SOFC cell construction technique has several risks, which are briefly discussed in Section 5. In the last section, the inherent risks and opportunities associated with fabrication are discussed, with a focus on the complexity involved in working with certain materials. Fig. 1 presents an outline of this review in the form of a flowchart.

S-SOFC is mainly about the configuration and functional lineup of active components in a single working SOFC application. SOFC can operate in dual modes, namely, the power generator and electrolysis modes. In short, this application is reversible. Research on S-SOFC is currently being studied actively. However, to develop a material applicable to various surroundings and environments, much improvement is needed to achieve a feasible condition. Many aspects need to be considered, from the choice of electrode materials and the method of production to the final fabrication of the cell. Each aspect is calculated and revised thoroughly;

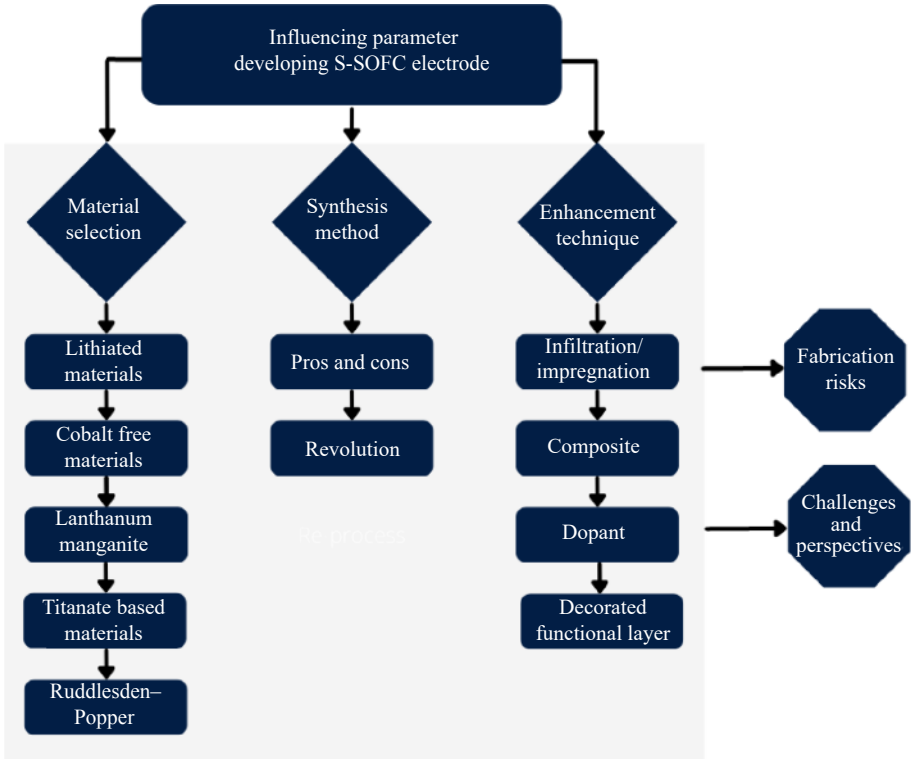

Fig. 1. Flowchart of the outline for influencing parameters in developing S-SOFC electrode.

however, issues between each process are beyond our control.

Meanwhile, S-SOFCs are soon to be operated in R-SOFC. The R-SOFC concept, which integrates SOFC and solid oxide electrolysis cell (SOEC) into a single unit, has been around for a few decades. When deployed as an SOFC, R-SOFC generates electrical energy from the reaction of fuel and air. Similarly, if integrated with an energy source, an R-SOFC in the SOEC mode (electrolysis) produces hydrogen (derived from water) or syngas (derived from the interaction of water and carbon dioxide). As the individual components of SOFC and SOEC still employ conventional materials such as YSZ as an electrolyte, lanthanum strontium manganese oxide (LSM) as the cathode, and Ni-based anode, their use raises concerns about the SOFC application.

This is because R-SOFC is conceptually and technologically dependent on the SOFC application, which continues to face common challenges and shortcomings. Thus, the S-SOFC is a part of the possibility and solution to realize the more advanced version of the R-SOFC, with less involvement of individual materials. This is where single materials are used for the electrode, which is believed to solve the concerning issues related to both electrode components. Fig. 2 explains the working mechanism of conventional SOFC and SOEC, which comprise the R-SOFC system. Thus, two devices are needed to complete the whole mechanism and later be incorporated into a single unit. The reactions at the electrode are represented using Eqs. (1)–(4).

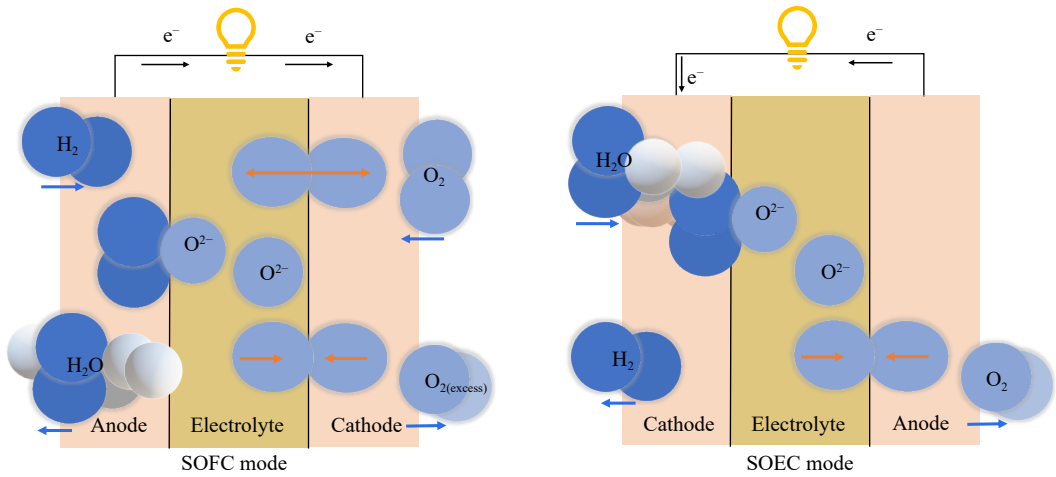

Fig. 2. Basic working principle of (a) conventional SOFC (power generation mode) and (b) SOEC (hydrogen/syngas production mode).

SOFC:

$$\text{Anode: } H_2 + O^{2-} \rightarrow H_2O + 2e^- \quad (1)$$

$$\text{Cathode: } O_2 + 2e^- \rightarrow O^{2-} \quad (2)$$

SOEC:

$$\text{Anode: } 2O^{2-} \rightarrow O_2 + 4e^- \quad (3)$$

$$\text{Cathode: } H_2O + 2e^- \rightarrow H_2 + O^{2-} \quad (4)$$

In contrast, S-SOFC consists of a single device that can operate in both modes. Because of this, research on the materials that make up S-SOFC has become the most pressing concern because the two distinct mechanisms are put into use. When a simple construction of a symmetrical design uses just one type of electrode, a single cell can function as both an SOFC and an SOEC device. While this configuration is run under both the SOFC and SOEC application mechanisms, the S-SOFC mechanism is comparable to that of the SOFC (power generation mode) as well as the SOEC (electrolyzer mode).

Basic S-SOFC components that involve two materials (electrode and electrolyte) mostly evolve from the base material, which initially is the main material for either cathode or anode. Optimizing various configurations, such as symmetrical SOFCs, can lower the operational temperature of SOFCs through enhanced electrochemical performance, improved catalytic activity, decreased activation energy, and better thermal management. The symmetrical design fosters efficient electrochemical reactions and synergy between electrode materials, enabling the fuel cell to operate efficiently at lower temperatures without compromising performance. Additionally, optimized thermal management ensures effective heat dissipation. These factors combined contribute to reducing the operational temperature while maintaining the desired power output and reducing production and running costs. The symmetrical configuration of SOFCs is an approach that can help lower the operational temperature. As mentioned earlier, symmetrical designs promote improved electrochemical performance and enhanced catalytic activity, which can result in more efficient reactions and reduced overpotentials. These factors allow the fuel cell to achieve its desired power output at low operating temperatures. In contrast, the goal of reducing the operational temperature is often driven by the desire to enhance cell durability, increase the life span of cell components, expand fuel options, and improve system integration. Lowering the temperature can help mitigate issues such as material degradation, thermal expansion mismatches, and thermal stress, which can occur at high operating temperatures. Therefore, reducing the operational temperature and adopting a symmetrical configuration can be seen as complementary design goals that are pursued concurrently. By optimizing the symmetrical design and other aspects of the fuel cell system, lower operating temperatures can be achieved while maintaining or improving the overall performance and efficiency of the SOFC.

The anode and cathode components each have their own distinct characteristics that enable them to operate within their respective working environments. Therefore, to create an "S-SOFC," one of the components needs to exhibit good electrochemical performance in both the anode and cathode environments. For example, in an S-SOFC built using the cathode material as the cell electrode, researchers need to ensure that this cathode material continues to demonstrate good catalytic performance in the anode environment [42]. Therefore, the lack of catalytic activity is considered the root of the S-SOFCs issue. Additionally, both the cathode and anode component deterioration was caused by the poisoning from sulfur and carbon, which occurred at the cathode and anode in rapid succession.

For example, cobalt-based perovskite materials are frequently adopted as cathodes for SOFC applications because of their good conductivity and electrochemical activity. However, commercialization of these materials is hindered by the material cost and thermal compatibility between components as well as sustainability reasons [38]. Hence, cobalt-free cathodes, such as $La_{0.5}Sr_{0.5}Mo_{0.1}O_{3-\delta}$, $La_{1-x}Sr_xFe_{0.8}Cu_{0.2}O_{3-\delta}$, and $Ba_{0.5}Sr_{0.5}Fe_{0.8}Sb_{0.2}O_{3-\delta}$-$Sm_{0.2}Ce_{0.8}O_{2-\delta}$ were introduced [39,43–45]. For anodes, conventional Ni-based materials were used. However, when operating in hydrocarbon environments, carbon and sulfur poisoning can also occur with these materials [46]. This poisoning can degrade cell performance or damage the cell structure [47].

The preliminary study on symmetrical electrodes mainly revolved around groups of materials, such as chromium manganite, lanthanum manganite, lanthanum chromite, and doped strontium titanate. These groups of materials were mostly studied for S-SOFC application. Doped strontium ferrite perovskites, such as $La_{0.6}Sr_{0.4}Fe_{0.9}Sc_{0.1}O_{3-\delta}$, $La_{0.3}Sr_{0.7}Ti_{0.3}Fe_{0.7}O_{3-\delta}$, and $La_{0.4}Sr_{0.6}Co_{0.2}Fe_{0.7}Nb_{0.1}O_{3-\delta}$, have been recently used as symmetrical electrodes [43]. These materials exhibit remarkable catalytic operation for oxygen reduction and fuel oxidation. The system durability at high operating temperatures has become a major obstacle to their application in S-SOFC [43]. One of the most approachable initiatives for developing a high-performance S-SOFC is by enhancing these materials through chemical and mechanical reactions to successfully achieve their commercialization [48].

Expanding the spectrum of materials research via chemical and mechanical processes entails providing an additional technique to obtain the desired material structure. These criteria are related to the material's morphological behaviors. The use of nano/micro materials has been a major development in the field of specialized electrode materials. Many of the above-mentioned materials were investigated using dopants. This procedure was carried out to evaluate the possibility of a dopant that may improve the overall performance of an S-SOFC. Using a dopant to improve an application's performance, in contrast, is a new task scope in which the approach itself is essentially another new material with a specified function in achieving a certain need. Therefore, clarity should be provided on how much attention should be focused on the basic material information related to the structure and synthesis process. The mentioned parameters are key to obtaining the ideal cermet electrode for the S-SOFC

application. These factors are important in ensuring the viability of a new electrode for S-SOFC such that the developed electrode fulfills the cathode and anode requirements.

2. Material selection

It is important to consider the many aspects that might have an effect, including the material selection, the synthesis process, the manufacturing stage, and the operational environment. Even earlier studies in the relevant literature focused on significant processes, which include material selection and processing conditions. Both characteristics are coupled to dispersion particles or connected microparticle networks to improve the electrochemical performance. As nanostructure materials remain stable over extended periods of time, there has been a continuing interest in their relevance, not to mention the many types of fuel (such as hydrogen, hydrocarbon, oxygen, etc.) that are employed during the operation process.

The S-SOFC configuration can be considered new because only a few electrode materials are reported to work well with this system; however, these symmetrical electrode materials are effective only at high temperatures. Consequently, for S-SOFCs to be economically competitive with conventional SOFCs, new materials with decent performance at intermediate temperatures must be explored and further researched. Material selection can be seen as the first stage in sorting the best feasible materials to work with S-SOFC based on the requirements of the electrode. The materials to be addressed in the next part are among those that are often employed in nano/micro applications because the beginning point for any research is dependent on the material behaviors itself, particularly for materials with excellent nano/microstructure. Therefore, a preliminary literature study on the material type developed or still in the preliminary study is critical in providing insight into the materials.

The perovskite group was utilized in the development of the material for the potential electrode and later parted on other based materials, such as lanthanum manganite, cobalt-free and lithiated materials, titanate-based materials, and to date, the Ruddlesden–Popper oxide-type materials. Perovskites represent a group of crystalline ceramic minerals whose composition is ABO_3. Oxygen vacancy is widespread within these materials and highly essential for ionic oxygen conduction. They cause oxygen ions to be transported selectively by means of a hopping mechanism where a gradient is found in the oxygen chemical potential. This condition can be achieved only if the oxygen ions have adequate thermal energy to pass the energy barrier for moving the ion. The total positive value of cations A and B is equal to the total negative value of the oxygen anion [49].

Fig. 3 visualizes the article publication trend related to electrode materials being researched for the past years until now (2019—2023). The keywords "symmetrical SOFC" and "reversible SOFC" were used under an advanced search for the title obtained from http://sciencedirect.com, as tabulated. Based on the chart, the research on the electrode materials for S-SOFC is still lacking, either for the technical or review publication to be compared with the oxide and proton-conducting SOFC (O^{2-}-SOFC and H^+-SOFC). Although using a single material that can function in two distinct contexts may save time, this does not apply to the preparatory investigations on the specific materials that must be conducted alongside the reported article for this application. Thus, in the next part, we will take a deep dive into the factors that matter most in designing a promising electrode for S-SOFC use.

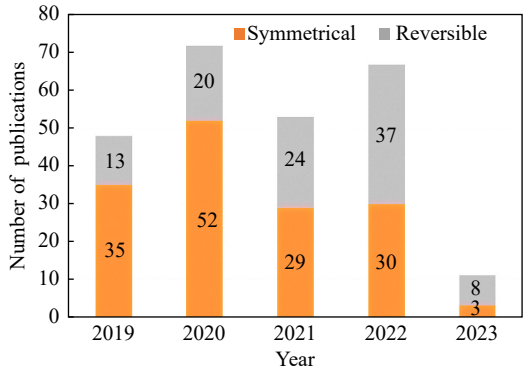

Fig. 3. Research article publication trend related to electrode materials being researched from 2019 to 2023.

2.1. Lithiated materials

To date, lithiated materials have been used widely in SOFC applications, either as a compound or a dopant, to enhance the material and overall application performance [50–52]. Lithium-containing oxide electrodes such as $LiNi_{0.8}Co_{0.15}Al_{0.05}O_2$ (NCAL), $LiNiO_2$, $LiNiCuZnFeO_x$, $LiNi_{0.2}Fe_{0.65}$-$Cu_{0.15}O_3$, $LiNiCuO_x$, and $Li_{0.3}Ni_{0.6}Cu_{0.07}Sr_{0.03}O_{2-\delta}$ show excellent catalytic activity as cathode and anode materials for low-temperature SOFCs [53–55]. NCAL was originally developed for Li-ion battery applications and incorporates layered cathodes of the $LiMO_2$-type as a working electrode material, referred to as mixed transitional metal (M)-layered oxides, or NCA [56–57]. It crystallizes in a hexagonal structure with the space group $R\bar{3}m$, comprising close-packed oxygen layers. The spaces between the oxygen layers are filled with lithium and transition metal (Ni, Co, Al) ions, which are randomly distributed within the Ni/Co layers, creating a disordered rock-salt-like structure. Within the oxygen layers, Li ions occupy two distinct forms of tetrahedral sites [56,58]. Moreover, lithium oxide has been used relatively as the sintering additive, especially in anodes. The explanation for this preference is that lithium has been previously identified as the competent dopant for procuring low-temperature sintering in ceria. This condition occurs because lithium oxide segregates to the grain boundaries by creating a liquid phase during the sintering stage, thereby enhancing its performance [59]. Li^+ also increases the ionic conductivity of an electrolyte material [60].

The lithium compound is indirectly added to the electrolyte materials because of the Li^+ migration phenomenon [61–62]. The lithium roles were discovered in a recent study where lithium-doped perovskite was used as the cathode

[63]. Thus, ORR activity was enhanced by 1.6-fold compared with the undoped cathode material. On this basis, an optimal amount of Li^+ was incorporated, resulting in relatively low electronegativity and contribution from the small size of Li [64]. The low electronegativity ensured a high concentration of oxygen vacancy, and a small ionic size induced Li^+ migration to the surface, thereby creating A-site deficiency at elevated temperatures [61,65]. Table 1 lists state-of-the-art SOFC components that use lithium compounds for various functions.

Table 1. Use of lithium in materials for an SOFC application

Ref.	Materials involved	Function	Component involved
[59]	NiO/GDC-GDC	Lithium salt (3wt%) as sintering aid	Anode
[61]	$La_{1.85}Sr_{0.15}CuO_4$-$Ce_{0.8}Sm_{0.2}O_{2-\delta}$ /$Ni_{0.8}Co_{0.15}Al_{0.05}LiO_{2-\delta}$ ($LSCO_4$-SDC/NCAL)	Prevent further reduction by hydrogen	Electrolyte and anode
[66]	$BaCe_{0.9}Y_{0.1}O_3$ (BCY) electrolyte	Improved ionic conductivity of the electrolyte	Electrolyte
[67]	$Gd_{0.1}Ce_{0.9}O_{1.95}$ (GDC)	Formed a three-phase composite cathode	Electrolyte and anode
[65]	$Sr_{1-x}Li_xFe_{0.8}Nb_{0.1}Ta_{0.1}O_{3-\delta}$	Forming A-sites deficiency	Cathode
[68]	$LiNi_{0.8}Co_{0.2}O_2$	—	Cathode material for triple ($H^+/O^{2-}/e^-$) conducting type
[69]	Li–Ni–M (M = Cu, Fe, Co)	—	Cathode material

The species infiltrated the electrolyte via diffusion induced by the chemical potential gradient overlaying the gadolinium-doped ceria (GDC) grains to build a composite electrolyte [70]. The assumption was that a space charge layer with cation elevation developed at the species interface, with an area of large oxygen vacancy proportion encircling it. This area potentially constituted a high-speed ionic transmission route in the newly formed electrolyte [71]. Therefore, the electrolyte's ionic conductivity was significantly enhanced. This finding is consistent with that from the previous research, which indicates that using NCAL as a current collector considerably enhances the performance of a single-component fuel cell with a mixed-oxide and ionic material composition [72]. Fig. 4 visualizes the lithiation mechanism, which involves lithium oxide electrode materials.

When combined with the samarium doped ceria (SDC) material, lithiated materials such as $Ni_{0.8}Co_{0.15}Al_{0.05}LiO_{2-\delta}$ (NCAL) are chemically compatible [73]. He *et. al* [74] verified that the improvement in ionic conductivity in a fuel cell with lithium-containing oxide as the electrode can be related to hydrogen on the anode side. NCAL/GDC/Pt (NCAL as anode) yielded a maximum power density of 37 mW/cm^2 at 550°C in H_2 compared with the cell using Pt as anode with 32 times performance difference. Verification via detailed characterization exhibited the presence of LiOH and Li_2CO_3 species in the NCAL anode over H_2 condition [75]. NCAL materials, because of their strong structural qualities for oxygen ion and proton ion conduction, were allowed to be used in a single-phase form rather than compositing with other ionic conductors [76]. These materials were recently employed as electrodes for symmetrical SOFC systems with triple charge conducting properties. NCAL electrodes perform as good

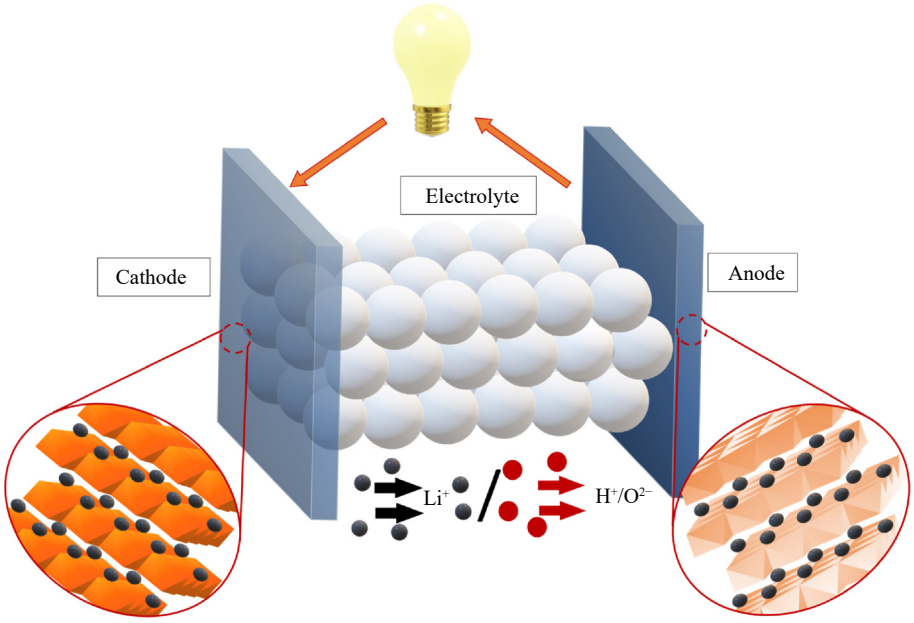

Fig. 4. Lithiation mechanism of electrodes in an S-SOFC application.

electrodes when used in both oxide and proton-conducting systems. The NCAL use as an electrode and a $BaCo_{0.4}Fe_{0.4}Zr_{0.1}Y_{0.1}O_{3-\delta}$-ZnO electrolyte results in a maximum power density of 643 mW/cm^2 at 500°C.

When the cell is operated in an air or H_2 environment, the NCAL anode reduces, and LiOH or Li_2CO_3 is generated, which is then drawn into the electrolyte. This technique densifies the electrolyte layer and increases the mechanical strength of the pellet. The technique also facilitates ionic transportation in the electrolyte and improves the catalytic performance of the electrode [77]. Till now, a layered structured $Li(Ni_{1/3}Co_{1/3}Mn_{1/3})O_2$ (LNCM) has been used as a symmetric electrode to boost the catalytic activity of symmetric electrodes for improved electrochemical performance. LNCM and NCAL have the same crystal structure and are both ABO_2 perovskite oxides. Li^+ inhabited the A-sites of both LNCM and NCAL, where it plays an important role in influencing the oxidizing state of Ni and catalytic activity [74,78]. The use of a high catalytic element such as nickel and cobalt provides LNCM advantages, as this electrode reduces into a nickel/cobalt alloy, also leading to $LiMnO_2$ formation during cell operation. The resulting alloy ensures good catalytic activity, whereas the byproduct $LiMnO_2$ promotes proton conduction [76].

The lithium oxide compound electrode serves as the air electrode (cathode) in lithium-ion batteries. The suggested NCAL materials have excellent electrode collector behavior and ensure a high catalytic activity. The addition of Ni/Co in NCAL induces the Schottky junction effect between (Ni/Co) created in the reduced NCAL and a semiconductor electrolyte, contributing significantly to high-performance fuel cells. The novel SOFC feature is examined wherein the anode and cathode are recognized as the n- and p-type areas separated by an ionic conducting electrolyte. The n- and p-type regimes correspond to anodes and cathodes, with the anode having a lower oxygen partial pressure and the cathode having a higher oxygen partial pressure. High electronic/hole conductivities are at least required for the anode and cathode, which are respectively placed in oxidizing and reducing atmospheres and are responsible for the hydrogen oxidation reaction and the ORR [79]. Therefore, narrow bandgap materials are required to allow adequate n-type and p-type conduction. In the S-SOFC, an electrode (anode) receives the fuel, which undergoes oxidation to produce electrons and ions, as is the case with most SOFCs. The electrons traverse an external circuit to reach the opposite electrode (cathode), where they combine with oxygen to generate oxide ions that return to the anode through the ceramic electrolyte [80]. At the Schottky junction, the electrons from the anode enter the cathode, encountering the built-in potential that impedes electron flow in the opposite direction. In the scenario involving the NCAL electrode, Li^+ migration leads to a greater metallic Ni presence in the L_xNO anode (x = 0.2, 0.4), potentially supplying more electrons to mitigate the Schottky junction effect. This process, in turn, enhances the overall current density and efficiency of the fuel cell [81–82]. A fresh approach to develop a potential electrode for fuel cell has been opened up by the numerous functions of lithium oxide or compound in fuel cell application. The most recent study used the $LiNiO_2$ oxide compound as the electrode and electrolyte, with $LiNiO_2$ as the electrode and $BaZr_{0.5}Y_{0.5}O_3$ (BZY)-$LiNiO_2$ as the electrolyte. Here, BZY is an excellent proton conductor; however, it has a sintering problem due to chemical disintegration in a reduced environment. The lithium oxide compound addition can help decrease grain boundary resistance and sintering temperature [82].

2.2. Lanthanum manganite

The well-known $La_{0.8}Sr_{0.2}MnO_{3-\delta}$ (LSM), which was developed by Siemens Westinghouse, is a pure electronic conductor and is among the previous material proposed as cathode materials for the SOFC application [83]. Although LSM recorded the longest lifetime in the SOFC operation, LSM still encounters the interfacial problem, especially between YSZ electrolytes [84]. LSM materials were found a long time ago and were also the first electrode candidates for SOFC applications. Despite the new material development, LSM-based materials are still considered the standard for continuous material improvement, using various techniques and approaches. Therefore, the performance of these materials, such as $(La_{0.6}Sr_{1.4})_{0.95}Mn_{0.9}B_{0.1}O_4$ (B = Co, Ni, Cu), $(La_{0.8}Sr_{0.2})_{0.9}Sc_{0.2}Mn_{0.8}O_{3-\delta}$, and $La_4BaCu_{5-x}Mn_xO_{13+\delta}$, is enhanced until the conductor becomes a mixed ionic and electronic conductor (MIEC) by means of doping at either the A- or B-site [85–87]. MIEC-type cathodes can extend the TPB, which is the active region, from the electrolyte-cathode interface to the entire electrode [88]. Strontium-doped LSM is another successfully developed material that is used to reduce the interfacial problem. This material exhibits sufficient electrical conductivity and good catalytic property, which is a mandatory property of an electrode, and a small TEC mismatch in the YSZ [89]. These values prove that this lanthanum manganite base is sufficient to serve as the cathode for S-SOFC. However, not much detail has been done on the fuel mode for these materials, in which further studies are needed, especially for the microstructure behavior as well as electrochemical properties.

Anode materials are intended to be chemically and mechanically stable in various conditions, especially when hydrocarbon gases are present at high temperatures. LSM was improved by doping technique with targeted elements that were not suited for the reduced condition as these elements were initially deployed as cathode materials. Fe or Mn is a common element extensively used in SOFC anode conditions to maintain the structure at high temperatures. Several perovskite manganites have been reported in the literature as having an oxygen vacancy order caused by hydrogen reduction in the atmosphere [90]. This scenario can be shown using the $La_8Mn_8O_{23}$ ($LaMnO_{2.875}$) and $La_4Mn_4O_{11}$ ($LaMnO_{2.75}$) examples. However, La/Sr manganites with the same crystal structure as $La_4BaCu_5O_{13+\delta}$ have previously been reported, with a composition of $(La_xSr_{1-x})_5Mn_5O_{13}$ (x = 0.1–0.3). As for

the cuprate, these compounds correspond to the order of four [$Mn^{3+}O_5$] pyramids and one [$Mn^{3+/4+}O_6$] octahedron-defining oxygen; however, the Mn oxidation state is still dependent on the La concentration [87,91]. Thus, the reason for using lanthanum manganite remains relevant despite the limitations, however, with further aid on structural improvement as well as with fabrication modification.

Lanthanum manganite-based materials, such as $La_xSr_{2-x}MnO_{4\pm\delta}$, which belong to the Ruddlesden–Popper (RP) family, were reported as electrodes for S-SOFC. The RP family was used because of its advantages in performance, such as being thermodynamically more stable under reducing conditions compared with conventional perovskites [92]. RP is a compound whose structure is the result of the perovskite-type and NaCl-type intergrowth. The general formula of RP is $A_{n-1}A'B_nX_{3n+1}$ (A & A′ = alkali, alkaline earth or rare earth metal | B = transition metal | n = octahedra's layers in the perovskites lookalike stack) [93–94]. $La_xSr_{2-x}MnO_{4\pm\delta}$ with composition x = 0.25–0.6 showed an excellent electrical conductivity as high as 35.6 and 1.9 S·cm^{-1} at 800°C in air and 3% H_2/Ar, respectively, thereby proving its feasibility to act as an electrode for the SOFC application [92]. Zhou *et al.* [86] studied the A-site deficiency in $(La_{0.8}Sr_{0.2})_{0.9}Sc_{0.2}Mn_{0.8-x}Ru_xO_{3-\delta}$, which can be used as an air electrode and a fuel electrode. Ru materials were used through infiltration rather than as a doping agent, where the ruthenium nanoparticle catalyst was exsolved on the $(La_{0.8}Sr_{0.2})_{0.9}Sc_{0.2}Mn_{0.8-x}Ru_xO_{3-\delta}$ surface in a reducing environment [86]. In the fuel cell mode, this material recorded a maximum power density of 318 mW·cm^{-2} at 50% H_2O/H_2 and 800°C.

Another significant condition as an electrode is that the electrode porosity must be in the 20%−40% range. This porosity range is significant, with enough porosity for electron flow and a large surface area for chemical reactions (oxidation and reduction). Aside from looking for approaches to improve the LSM materials by doping, composite, and synthesis methods, the morphological structure enhancement of the synthesis LSM is of interest. Gager *et al.* [95] and colleagues use the replica method to produce a reticulated porous lanthanum strontium manganite structure. The following are the characteristics of replica foam [95]: (1) Control the foam structure for improved performance and efficiency. (2) Design structures with dual-scale porosity to improve heat transmission while increasing the surface area. (3) Increase control over the microstructure.

Although the LSM ceramic foam was created for solar thermochemical hydrogen generation, the reduction process studied throughout this application can be considered for S-SOFC applications where hydrogen is one of the fuel sources. The result was developed LSM ceramic foam with micron-sized growth as well as grain growth limitation of about 1 μm. Nevertheless, synthesis parameters, such as the polymer additive calcination toward this LSM, must be considered, as also the possibility of manganese species degradation.

Deploying lanthanum manganite-based materials in unique environments is an important measure to obtain competent electrode candidates for S-SOFC. This material is desirable because it has the ability to reverse at least almost the same structure when undergoing reduction on supplying an oxidant. The reason is that it is one of the alternatives to counter possible carbon coking and chromium and sulfur poisoning. A study of the LSM-based materials aimed to prepare this material for R-SOFC application, which is one of the concerns in S-SOFC, where this LSM was conducted for multiple chromium poisoning cycles. Utilizing a novel technique called *in-situ* electrochemical cleaning, which serves as a mitigation method for chromium poisoning, the LSM-YSZ material experienced a significant recovery of its cathode portion from the poisoning effects. This process prolongs the overall SOFC system lifetime [96].

2.3. Cobalt-free materials

The need for excellent catalytic activity, mainly linked to cobalt, was found to be best fulfilled by making cobalt the primary element in the SOFC electrode. When used in hydrocarbons, Co has been proven to prevent coke formation, especially when the neighboring element of Ni was used as an electrode. The cathode material evolution is highly dependent on Co. Cobalt-containing materials, such as $La_{0.5}Ba_{0.5}CoO_{3-\delta}$, can exhibit high electrical conductivity, however, and can suffer from fast cell degradation and high TEC, leading to low compatibility with the electrolyte material [97–99].This situation affects the chemical stability and the overall cell performance while running at a high temperature because of high redox activity [42]. Thus, cobalt-free materials were introduced to cope with these issues faced by cobalt-containing materials.

Cobalt-free materials as promising electrode materials, especially at low operating temperatures, are widely investigated because they exhibit excellent properties, such as good electrocatalytic activity and thermal stability under fuel cell operating environment in addition to good TEC between the electrolyte [100]. Cobalt-free iron is a promising material that exhibits excellent properties, including the TEC feature to operate under an intermediate SOFC environment [26]. Previous studies used cobalt-free iron-based materials, such as $Sm_{0.95}Ba_{0.05}Fe_{0.95}Ru_{0.05}O_3$ (11.4×10^{-6} K^{-1}) and $Pr_{0.5}Sr_{0.5}Fe_{1-x}Cu_xO_{3-\delta}$ (14.4×10^{-6} K^{-1}), measured at room temperature up to 100°C and showed a lower TEC value compared with cobalt-based materials [71–72]. For the S-SOFC application, cobalt-free-based material, $La_{0.5}Sr_{0.5}Fe_{0.9}Mo_{0.1}O_{3-\delta}$ (LSFMo), was evaluated as the electrode for S-SOFC and tested for stability in 5% H_2/Ar and H_2 [43].

Fig. 5 shows the report from Cai *et al.* [43] on the relevance of the X-ray diffraction (XRD) study of the reduced and unreduced conditions for LSFMo. This report highlighted the potential of this material as an electrode for S-SOFC. XRD analysis can identify any change in structural and phase orientation that may affect the overall cell performance. The unreduced LSFMo samples had a cubic form structure with a space group of $Pm\bar{3}m$. The response peak after the reduction shows no further peak, suggesting that there is no impurity

phase precipitation present after the reduction process. However, as seen in the inset figure, the peak shift phenomena can be attributed to the Fe/Mo cation reduction to their lower valence states. Given that SOFC anodes are often needed to run in high H_2 fuels, the LSFMo stability under pure H_2 must be identified. Undoubtedly, only small amounts of the $LaSrFeO_4$-layered perovskite phase were discovered in the LSFMo reduced in pure H_2 at 800°C, whereas no $LaSrFeO_4$ trace was detected in the 750°C reduced sample. This suggests that the LSFMo electrode has high redox stability at temperatures lower than 800°C. To avoid phase separation/precipitation in the anode, the SOFC operating temperatures, using LSFMo as both the cathode and the anode, should be kept below 800°C. SOFC features, such as structural and chemical stability and electrical behavior, were presented in designing a promising electrode for S-SOFC [43].

Yang *et al.* [101] demonstrated another cobalt-free material as the future electrode candidate for S-SOFC $Ba_{0.5}Sr_{0.5}Fe_{0.8}Cu_{0.1}Ti_{0.1}O_{3-\delta}$ (BSFCuTi) by comparing the features of the undoped version of $Ba_{0.5}Sr_{0.5}Fe_{0.8}Cu_{0.2}O_{3-\delta}$ (BSFCu). The electrical conductivity studies for this material exhibited accentuate the notability of sufficient conductivity. However, the low electrical conductivity exhibited by these materials, where the preferred is more than 100 $S \cdot cm^{-1}$, proves that achieving a reasonable power output by adapting the microstructure morphology is still possible [102]. Pure Fe-based cathodes, in contrast, are not as active as Co-based cathodes and require external-cation doping, such as Nb^{5+}, Ta^{5+}, Sn^{4+}, Sb^{3+}, In^{3+}, Ni^{2+}, and $Mn^{4+/5+}$, to stabilize the lattice structure and increase electrocatalytic activity with extremely disordered-structure. Although cubic BSCF demonstrated excellent ORR activities, structural stability is a challenge [95].

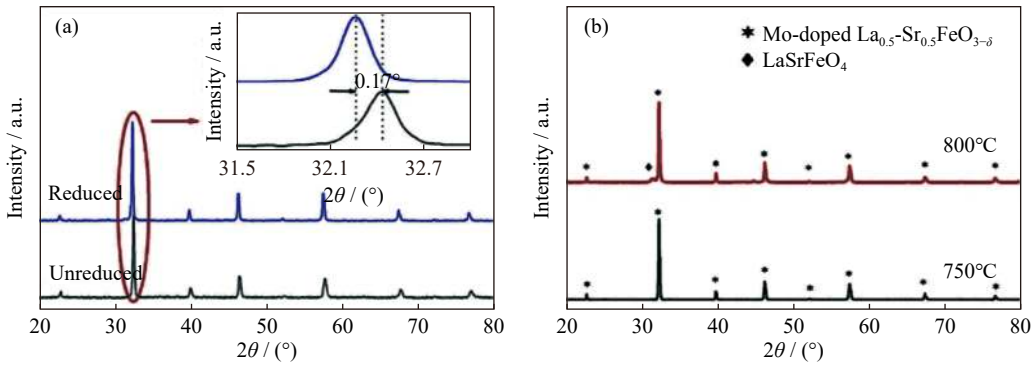

Fig. 5. XRD patterns of reduced and unreduced LSFMo samples under (a) 5% H_2/Ar and (b) H_2 [43]. Reprinted from *Electrochim. Acta*, 320, H.D. Cai, L.L. Zhang, J.S. Xu, *et al.*, Cobalt-free $La_{0.5}Sr_{0.5}Fe_{0.9}Mo_{0.1}O_{3-\delta}$ electrode for symmetrical SOFC running on H_2 and CO fuels, 134642, Copyright 2019, with permission from Elsevier.

2.4. Titanate-based materials

Titanate-based materials, which are frequently used in anode materials, are now being intensively studied for the future electrode in S-SOFC. Strontium titanate ($SrTiO_3$) is one of the candidates with potential because of its strong anodic and cathodic stability, moderate thermal behavior, and significant carbon deposition and sulfur poisoning. Second, at 1400°C, $SrTiO_3$ has been shown to be chemically stable with various electrolytes such as $Zr_{0.82}Y_{0.16}O_{1.92}$ (YSZ), $La_{0.9}Sr_{0.1}Ga_{0.8}Mg_{0.2}O_{3-\delta}$ (LSGM), and $Ce_{0.9}Gd_{0.1}O_{1.95}$ (CGO) [103]. Following the trend of using titanate-based materials as the primary components, various techniques have been investigated to enhance the efficiency of these materials. Most studies use a dopant and composite approach to produce a certain potential that qualifies it as an electrode (anode and cathode). For example, the oxygen reduction process requires the co-doping of Pr onto the A-sites of $SrTiO_3$. Meanwhile, the electrolyte composite works to promote ionic conductivity while decreasing thermal incompatibility at the substrate contact. Despite its reasonable performance, $SrTiO_3$ is still inferior to existing electrodes because of low ionic conductivity and electrocatalytic activity.

Titanate group-based materials have shown to be promising S-SOFC-based materials, as evidenced by their emergence as interconnect materials. Because few materials are suitable for use as interconnect materials. This is owing to the titanate-based material's exceptional electrical conductivity in reducing atmospheres, remarkable redox stability, and good thermal expansion matching to other components being applicable to the anode side [104]. Miao *et al.* [105] worked on $Sr_{0.88}Y_{0.08-x}Yb_xTiO_3$ and $Sr_{0.88}Y_{0.08}Ti_{1-x}Yb_xO_3$, which were produced by Yb^{3+} doping in the A-site and B-site of $Sr_{0.88}Y_{0.08}TiO_3$ perovskite, respectively. Due to the strong carbon deposition resistances, the performance using $Sr_{0.88}Y_{0.06}Yb_{0.02}$–$TiO_3$ anode exhibits superior stability when operated in CH_4. This materials' performance demonstrated that titanate-based materials are another developing all-rounder material for future SOFCs.

Looking back to the main criteria of both anode and cathode materials, where the materials employed must surpass 100 $S \cdot cm^{-1}$ to provide good power performance by the SOFC operating system, the $SrTiO_3$ electrical characteristics are among the top tiers. While $SrTiO_3$ is currently being researched as an anode for SOFC, research into the cathodic environment is gradually increasing. $SrTiO_3$ has outstanding dielectric characteristics and is a great semiconductor, allowing this modified titanate-based material to be used as an

MIEC cathode that supports both ionic and electronic conduction [106]. Strontium titanate perovskites are known to be exceedingly stable and coking resistant, and La doping at the A-site (i.e., over Sr) generates oxygen-rich planes and enhances both ionic and electrical conductivity. It was discovered that 20% La doping is the optimal amount for maximum conductivity, while Cl doping nearly doubles oxygen mobility, which is critical for any SOEC electrode. $La_{0.2}Sr_{0.8}TiO_3Cl$ was evaluated as a possible cathode catalyst for these reasons [107].

2.5. Redox-reversible typed materials (Ruddlesden–Popper types oxide materials)

S-SOFC electrodes can be primarily obtained from cathode or anode materials. RP materials were initially introduced in 1958 by S.N. Ruddlesden and P. Popper with the general formula $A_{n+1}B_nO_{3n+1}$. RP materials began from the perovskite derivation and then progressed to double perovskites. These materials perform well as SOFC cathode materials. The peculiar structure comprises the $n$$ABO_3$ perovskite layers sandwiched between two AO rock-salt layers. Second, the number of perovskite polyhedral units sandwiched controls the material phase and this structural resemble RP phase materials to perovskites [108].

Layered K_2NiF_4-type $Ln_2NiO_{4+\delta}$ (Ln = La, Pr, Nd) nickelates, the first RP kind of oxide materials, have particularly exceptional behavior as cathode materials, for instance: high surface exchange kinetics; increased oxygen ion diffusivity; adequate electrical conductivity; moderate TECs. Unlike other oxide forms, RP-type materials may accommodate oxygen interstitial deficiencies in the AO layers, resulting in a hyper/hypo stoichiometric state for their oxygen concentration. This process appears to have an impact on oxygen transportation characteristics because oxygen ion migration can occur via a mechanism associated with oxygen vacancies or interstitials [109]. RP oxides, such as rare earth nickelates with the chemical formula $Ln_{n+1}Ni_nO_{3n+1}$ (Ln = La, Nd, Pr), are among the RP families that have received substantial research because of their peculiar structure and significant ORR activity. Meanwhile, Pr_2NiO_4 has the highest oxygen surface exchange coefficient (K^*), the lowest diffusion coefficient (D^*), and the lowest polarization resistance among the Ln_2NiO_4 oxides. It also has the maximum oxygen permeability, the lowest TEC (14×10^{-6} K^{-1}) and is compatible with most electrolytes [110].

While working on the electrode for the S-SOFC materials, Wu *et al.* [111] reported that growing nanoparticles on the perovskite electrode surfaces frequently results in structural modifications. An example can be seen from the $LaSrFeNiO_6$ anode as reported in Ref. [111], in which at first the anode resembles a perovskite material and later is transformed into an RP-type oxide material. The RP-type anode materials require extensive improvement, mostly in terms of structural changes because of the previously described modification approach. As the sophisticated system of RP-type oxide materials, the chemical structure of the chosen candidate must have a favorable stability in reducing environments [85].

A RP layer-structured oxide, $La_xSr_{2-x}MnO_{4+\delta}$ ($LSMO_4$, x = 0.25–0.6), is recently proposed as the electrode for symmetrical SOFC because of its high structural stability in both oxidizing and reducing atmospheres. The first serial A_2BO_4 RP-type $LSMO_4$ can be considered an alternate rock-salt and perovskite layer stake. The rock-salt layers may hold many interstitial oxygen ions; however, the perovskite layers can induce oxygen vacancies. Therefore, unique oxygen diffusion capabilities have been demonstrated, making RP-type materials suitable for use as electrodes. Moreover, $LSMO_4$ is electrically conductive in both reducing and oxidizing environments [112].

For S-SOFC applications, typical RP material-type electrodes have been examined. Nevertheless, several materials with redox-reversible stability have also been studied. Redox reverse stability indicates that the structure is unstable in a reducing environment; however, the structure can be reversed by calcining in the air [113]. Nonetheless, electrode electrochemical activity still must be improved. As a result, methods for decorating an electrode surface, such as infiltration, deposition, and exsolution, have recently received a lot of interest. Among them, *in-situ* growing nanoparticles on the perovskite-type oxide surface is regarded as a simple and cost-effective method of producing highly active catalysts [114].

3. Revolution of common synthesis method: Pros and cons

To create technologies that can meet the global energy demand, it is essential to improve the overall SOFC application performance. The synthesis process is the next in line of important stages toward full-scale S-SOFC implementation after material selection. Another element to figure out is what materials will be used for the electrodes in an S-SOFC, which will, in turn, influence which synthesis process will be used. It is possible that, as the analysis process progresses, some deterioration can be discovered. A certain precursor material performance for an SOFC application is determined by the material processing or synthesis. The characteristics and shape of the materials derived from the electrode materials and all the components involved in SOFC application are determined by the synthesis process used to produce them. The multiple possible synthesis methods, however, are always narrowed down by the amount of work required to finish the process, cost-effectiveness, and final product features. Several common approaches to material synthesis are discussed and reviewed, along with the pertinent details. Despite the method's apparent commonality, its practicality, durability, and high-tech capacities set it out as a distinguishing aspect. Thus, this part provides a fresh perspective and solutions to the issues that have plagued more conventional approaches in the past.

3.1. Mechano-chemical reaction

The conventional solid-state method is a cost-effective yet time-consuming and laborious method because it includes

manual grinding of the precursor raw materials. The solid-state method is more attractive because of its eco-friendly, green, and facile characteristics compared with other synthesis methods. This method has been used in most nanomaterials, such as composites, metal oxides, and inorganic materials [115]. The raw materials used were calculated stoichiometrically and ground using mortar and pestle for a certain time duration. The ground powder quality was determined by observing its texture, and the ground powder was later heat treated. A continuous concern toward this valuable processing method highlighted this matter. Wang *et al.* [115] proposed a novel solid-state chemical reaction to synthesize a composite TiO_2/anatase oxide. The raw materials used were all analytically pure, mixed, and ground through ball milling. The modified part is where the obtained powder was warmed with an aqueous bath at 70°C overnight and then calcined. The calcined materials were processed, and the powders were washed with deionized water and dried. This study suggested a new method to produce TiO_2(B)-based composite oxide materials. The additional step of this modified specific settling rate (SSR) was adopted to improve the physical and chemical reactions.

Conventional SSR may involve the physical reaction of the mixture yet not the chemical reaction. This condition is where the additional step sequence in the aforementioned process is used for a better end product. Thus, the physical and chemical reactions of the raw materials can be fully optimized for better performance by implementing this modified SSR. Pineda *et al.* [116] worked on a double perovskite-type compound namely $REBa(Co,Mn)_2O_{5+\delta}$, $NdBaMn_2O_{5+\delta}$ that is synthesized via solid-state reaction. This complex phase structure, RE/Ba sequence, can stabilize the oxygen vacancies in the lanthanide plane [117–119]. Preheating treatment steps were performed for the required raw materials to synthesize $NdBaMn_2O_{5+\delta}$. Nd_2O_3 was treated at 200°C in a vacuum furnace before physically mixing with other raw materials [116].

Ball milling is a simple, one-step method that is introduced to physically improve and modify the raw material microstructure. This method is well known, especially for mixing powders and dispersing metals and mixtures [120]. The process simply consists of raw materials that are stoichiometrically calculated and ball milled (e.g., zirconia ball) with a particular time duration and rotational speed. This method involves dry and wet milling. Wet milling is a modified technique that involves a solvent to improve the reactivity and purity of the mixture [121]. The high deformation and relatively low temperature are involved in addition to the heat generated by the rotating system. High-energy ball milling is introduced and widely used because it changes the raw material size and microstructure.

High-energy ball milling is a method used to obtain ultrafine materials, where the raw materials are continuously subjected to a relatively high-speed grinding ball milling in a specially designed vessel [122]. Particle annihilation in cold mode grinding occurs repetitively because of ball milling on crushing the powders [123]. This method reduces the agglomeration and intensifies the homogeneous distribution of alleviated particles to nano-size as the end product [124]. The optimization of high-energy ball milling parameters to synthesize an oxide dispersion powder strengthened by an alloy type [125]. The varying parameters are rotational speed and milling time, where the optimum results for the 10:1 ball-to-powder ratio are 1000 r/min for 6 h, resulting in a narrow particle distribution (5–33 μm).

3.2. Sol–gel method

The sol–gel method uses the mixture combustion by using citric acid as a fuel to form the end product in a gel form. This method is highlighted because it is convenient, although it is not included as a single-step processing method. This method obtains end products with nanopowders, fibers, nanotubes, and thin films, including those with complex compositions at low synthesis temperatures [126]. One such process is often used in ceramic and powder production because of its excellent tolerance to contamination, reduction, oxidation, and degradation mechanisms [127]. This approach does not include melting or sintering powders to manufacture ceramics but rather uses a reactive precursor-containing substance for forming a colloid composed of a metal or metalloid element surrounded by various ligands. This method also exhibits the upper hand in the ability to control the composition, morphology, and microstructure, which is the top priority in synthesizing the powders for electrodes in SOFC applications.

The potential of the sol–gel process to offer new sophisticated functional materials based on diverse micro and macrostructures has been recognized by researchers. Perovskites were mostly synthesized through a modified sol–gel method, where the process was assisted by additional ethylene and activated carbon as chemical additives [128]. Badge and Deshpande [129] synthesized bismuth titanate via solid-state and sol–gel reactions. They proved that the ceramic obtained from the sol–gel method and sintered at 1000°C for 3 h exhibited the highest density compared with the solid-state reaction method. Mateos *et al.* [130] verified the synthesis of high-purity nickel oxide via the modified sol–gel method using nickel acetate, citric acid, and ethylene glycol as precursors. The pre-calcined powder particle size is approximately 50 μm and can be as low as 10 μm after an hour of calcination at 800°C. The sol–gel method should be considered a potential method to synthesize the potential electrodes for S-SOFC application.

Despite its advantages, this approach also has drawbacks. The following are the benefits of the sol–gel approach, as highlighted by Modan and Plăiașu [131]: (1) the potential to manufacture high-purity end products because of the organometallic precursor of ceramic oxides that can be dissolved in a specific solvent and hydrolyzed to a gel with a highly regulated composition; (2) lowering the sintering temperature to approximately 200–600°C; (3) a simple, cost-effective, and fast approach for producing high-quality coverage.

Regardless of the benefits highlighted, each synthesis technique has its own drawbacks. For example, the hydrox-

ide-based metal and additive inclusion in the precursor mixture produces excess hydroxyl and carbon residue. Some materials even undergo double calcination to get desirable materials in the end. Another disadvantage of using this approach is the lengthy processing time. Several studies have even shown that the extended processing time may have an impact on the purity of the final product [132]. The next thing to consider is the possibility of fine holes forming because of the contraction that happens during the processing stage, as well as the usage of organic solutions that can be poisonous.

3.3. Glycine nitrate combustion method

Glycine nitrate combustion (GNC) is driven by the advancement of a homogeneous chemical as well as spontaneous combustion, resulting in a shorter calcination period with a crystalline final product [133]. The size and the morphology of particles synthesized by this method crucially correspond to the main parameters, which are the fuel-to-oxidant ratio, cation concentration in the mixture, and rates of gases that are released during combustion [134]. Thus, these parameters should be highlighted to obtain a product with optimum quality and effective combustion. The amount of fuel (glycine) used in this procedure must be determined analytically to ensure that just the minimum amount of fuel is required to effectively combust the precursor nitrate compound. Amaraweera *et al.* [134] demonstrated that the ratios used in the mixture influenced the phase and performance of the materials.

The simultaneous-auto combustion that occurred during the processing technique afforded this procedure an advantage in producing nanomaterial-sized particles. Given the above benefits of the GNC approach, it was employed to synthesize electrodes and electrolyte components [76,135]. The glycine-cation ratios were the most critical aspect that was addressed. The glycine-cation ratio stoichiometric calculation emphasized the characteristics and cation number of each metal employed in the compound. To date, GNC has been improved by using microwave-assisted combustion because this modified method initiates the combustion reaction at a fast rate and with uniform energy, in addition to the high crystallinity and purity of the end product [136]. Technically, microwave-assisted GNC is fast, practical, easy, simple, and energy-saving. Compared with conventional combustion using a hotplate, microwave energy is used to channel a specific amount of electromagnetic energy and directly convert this energy into heat [137].

Unfortunately, both the conventional and advanced methods of GNC have complications during combustion. Even though the glycine-cation ratios were precisely determined, the reactivity of the specific cation may differ. Certain compounds containing highly reactive elements, such as cobalt, nickel, and manganese, do not promote smooth combustion. Instead, the combustion occurs with a small spark and quick burning, resulting in the formation of ashes that scattered. The advanced approach, which uses a microwave to promote combustion, stays the same. What make it worse is the spark created may have even blown the microwave oven (commercial microwave oven), and certain compounds may have even blasted out the microwave. These situations result in a significant loss of precursor materials. Hence, using this strategy is beneficial with all the benefits given forth; however, further study on the materials and appropriate glycine-cation ratio must be done.

3.4. Benefits and drawbacks of advanced methods

Considering alternatives to or improvements on the traditional process of synthesis may serve as a great possibility; however, it may also bring about unfavorable effects. Whether it is for large-scale manufacturing or small-scale production, it is necessary to take the most cutting-edge approach into account to boost the efficiency. Second, an additional synthesis phase is an important consideration that needs to be given attention since it has the potential to restrict the primary objective of having an S-SOFC configuration that can be implemented, which is to simplify all aspects as much as possible. The benefits and drawbacks of the more sophisticated approach are summarized in Table 2, which follows the previous discussion of the method.

Table 2. Advantages and disadvantages of advanced synthesis method

Method	Advantages	Disadvantages
Solid state	Simple process	Non-homogenous and large particle size
Ball milling	Effective	Time-consuming, particle distortion
Sol–gel method	Large scale production	Multiple steps
Glycine nitrate combustion	Homogenous and fine particle	Excessive combustion and can be hazardous

4. Materials enhancement method

SOFCs are commonly operated at temperatures over 800°C to maintain adequate catalytic activity and acceptable ionic and electronic conductivity. High working temperatures present issues in terms of sealing, sluggish response to start-up and cooling, high overall system cost, and rapid material deterioration. SOFCs operating at intermediate temperatures (IT-SOFC) (500–750°C) are desired to address the problems. The performance and output power of SOFCs in IT temperature ranges are heavily dependent on the ORR catalytic activity of cathode materials. There are two key phases in the ORR process: reducing oxygen at surface active sites and transporting oxygen ions away from the sites. To improve electrode performance, there are two approaches: inventing novel materials and modifying the existing cathode materials.

4.1. Electrode infiltration/impregnation

In addition to material selection, numerous material processing processes were investigated for electrode improvement. It has been revealed that co-synthetic composited electrodes outperform standard mechanical mixing composited electrodes in terms of performance [32]. Another strategy for improving electrode performance is electrode infiltration/impregnation. This approach, which is frequently employed on existing electrode materials, yet still lacks oxidizing and reducing activity. Several advantages of this method are as follows: (1) Surface coatings can be made from a variety of active elements (including materials with high thermal mismatch). (2) Upon surface infiltration, both the surface composition and the surface structure can be varied. (3) This approach enables a moderate heat treatment temperature (900°C) by preventing mechanical mismatches produced by crystal particle coarsening and reducing contacts between the coating material and the substrate. (4) Infiltration can improve cathode durability and contamination tolerance. (5) Last but not least, this method is capable of producing a particular metallic nano-catalyst.

In the development of S-SOFCs, optimization of the perovskite oxide hydrogen electrode microstructure for enhanced performance has been widely used. To effectively improve electrode performance, nano-catalysts, which can be highly-performed metallic catalysts such as Ni, Co, Ag, Cu, and Ru or oxide catalysts such as cerium oxide (CeO_2), Gd-doped CeO_2, $PrBaMn_2O_{5+\delta}$ (PBM), and $Sr_2Fe_{1.5}Mo_{0.5}O_{6-\delta}$ (SFM), have been commonly introduced into porous oxide electrodes to form a nanostructured electrode. This approach has demonstrated several benefits in terms of increasing electrode performance, such as decreasing resistance and preventing electrode deterioration [138].

Several researchers employ direct composition, co-synthesis, and infiltration processes to improve the ionic conductivity of $La_{1-x}Sr_xMnO_3$ electrodes. Among these approaches, the infiltration procedure may improve the effective reaction sites by incorporating nanoparticles into the electrode scaffold, and TEC mismatching between various components could be prevented. Ionic conductors are used as potential materials for infiltration in the early stages. According to Vafaeenezhad *et al.* [139], $Sm_{0.2}Ce_{0.8}O_{1.9}$ (SDC) infiltration improves the electrochemical reaction not only in the SOFC mode but also in the SOEC mode. Another feasible way to improve the electrochemical performance of LSM oxygen electrodes is the infiltration of MIEC materials. To date, the agglomeration of nanoparticles at high operating temperatures due to high surface energy has been the key obstacle in the long-term steady operation of infiltrated electrodes. Co-infiltration of sintering inhibitors and catalysts has been explored to prevent catalyst particle coalescence [140]. Fig. 6 visualizes the simple infiltration/impregnation and possible scenario of the formed particles onto the electrode. The first scenario is the formation of well-dispersed nanoparticles on the surface of the electrode, and the second scenario is the electrode particle being encapsulated by the impregnation/infiltration materials.

4.2. Composite (electrode–electrolyte)

Developing a new electrode material that possesses sufficient ionic conductivity is another research trend to ensure its viability to operate under S-SOFC operating temperature [141–142]. However, several electrode materials with excellent catalytic activity, such as $La_{0.6}Sr_{0.4}CoO_{3-\delta}$, $SrCo_{0.7}Nb_{0.1}Fe_{0.2}O_{3-\delta}$, and $Sm_{0.5}Sr_{0.5}CoO_{3-\delta}$, have been discovered in previous years [143–145]. Cobaltite or ferrite oxides are either thermally incompatible or chemically reactive to the electrolytes despite the highly catalytic activities involved in response to oxygen reductions and their low polarization resistances. Moreover, at lower temperatures, fuel cell power densities decrease noticeably owing to slow kinetics for electrochemical processes in the electrodes, particularly oxygen reduction events in the cathode. For example, large polarization resistance was found for Sr-doped $LaMnO_3$ (LSM), the frequently used cathode material for SOFCs with YSZ electrolytes [146]. Commonly used composite material Ni–YSZ for anode and cathode certainly exhibits high electrical conductivity and excellent catalytic activity. However, this material possesses a relatively low tolerance toward the coking phenomenon in addition to the oxidation of Ni particles when

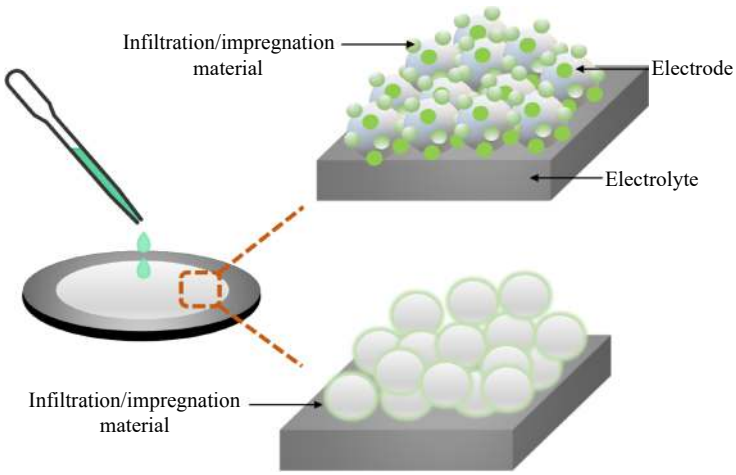

Fig. 6. Possible scenario of impregnation/infiltration particle after heat treatment.

operated in a CO_2 environment [147–148]. These major problems may degrade the cell performance and lead to poor cell stability, which are important aspects of operating the S-SOFC. Thus, combining the highly ionic conducting material with other materials, such as GDC electrolyte and $Sr_2Fe_{1.3}Co_{0.2}Mo_{0.5}O_{6-\delta}$, becomes a solution to overcome the disadvantages [44].

The data presented by Yu *et al.* [149] summarized that electrolytes, such as YSZ and LSGM, are among the commonly used electrolytes because of their good electrolyte domain at various operating temperatures and oxygen partial pressure. Electrolytes such as doped ceria, ceria carbonate, and proton-conducting electrolyte are also used; however, their adoption is not that extensive compared with the previously mentioned electrolytes. Xu *et al.* [150] reported a composite electrode $La_{0.3}Sr_{0.7}Ti_{0.3}Fe_{0.7}O_{3-\delta}$ composite with CeO_2. This electrode was synthesized through infiltration and analyzed thoroughly for S-SOFC at multiple ratios of CO/CO_2 under operating temperatures varying from 700 to 850°C. In the fuel cell mode, this material exhibited the maximal power density of 437 $mW \cdot cm^{-2}$ at 800°C, fueled with 70% CO and 30% CO_2, which was sufficient for this operation. Degradation may occur because of the agglomeration in the microstructure of this material.

4.3. Dopant

Introducing dopants to particular base materials typically achieves its full performance by varying concentration doping levels, synthesis techniques, as well as fabrication techniques [151]. Perovskites are a kind of material that has an ABO_3 structure. Perovskite and its derivatives have been considered one of the most promising SOEC cathode materials because of their high catalytic activity and stability. The enhancing strategy involves incorporating certain elements into the A- or B-site of these structures to highlight specific qualities. Catalytically active transition metals like Rh, Pd, Pt, Fe, Ni, and Co are substituted in the perovskite lattice as a solid solution under an oxidizing atmosphere and then exsolved as metal nanoparticles (NPs) anchored on the perovskite surface under reducing atmosphere. This is a workable strategy for manipulating catalytic active sites. In SOEC, SOFC, and other heterogeneous catalytic processes, the perovskites undergoing redox exsolution have distinctive catalytic activity, thermal stability, and coking resistance [152].

Perovskite oxides are MIECs that are commonly adopted as cathode and anode materials in SOFCs. Perovskite oxides based on $LaCoO_3$ are being investigated as prospective cathode materials for SOFCs; the insertion of Sr on the A-site in $LaCo_3$ can further boost catalytic activity because of an increase in oxygen vacancy concentration. Meanwhile, partial substitution of high or fixed-valence elements (such as Ni, Fe, Mo, or Zn) on the B-site can significantly improve the catalytic activity of perovskite oxides in an oxidizing environment. When the perovskite structure is doped with the appropriate quantity of other elements, there is essentially no distortion. Also, the radius of the doping cation should be comparable to that of Co_3 [81].

A lower reduction temperature, according to Li *et al.* [81], is correlated with a decrease in the binding energy between the metal and oxygen ions in the perovskite structure. This effect is attributed to Rh's higher electronegativity (2.28) compared to Ti's (1.54), which might influence the redox capacity of Rh-doped SYT catalysts, enhancing catalytic activity toward electrochemical reactions [153]. The structural stability and catalytic activity of the perovskites are attributed to the alkaline earth and transition metal ions occurring at the A and B sites, respectively. Nevertheless, the doping technique at the A-site, which involves replacing trivalent lanthanide ions with divalent alkaline earth ions, is frequently used to enhance the electrochemical performance. According to Kannan *et al.* [154], this substitution in the perovskite-type $Nd_{0.75}Sr_{0.25}Co_{0.8}Fe_{0.2}O_{3-\delta}$ creates extrinsic oxygen vacancies, considerably boosts the cathode's overall performance by contributing the oxygen molecules' reduction sites, and then migrates the oxygen vacancies. In fact, the chemical and electronic states of B-site transition metals can directly influence how the ORR activity of perovskites is impacted. More lanthanide ions at the B-site can enhance the perovskite's lattice parameters and free volume, which is frequently linked to higher oxygen ion mobility and lower activation energy. A more significant benefit of such low activation energy is the enticing ORR activity at low operating temperatures. Moreover, the newly added B-site lanthanide ions with larger ionic radii achieve a lowered tolerance factor close to 1.0, resulting in a perfect cubic symmetrical structure with a rapid oxygen bulk diffusion rate and surface oxygen exchange kinetics [155–156].

4.4. Decorated functional electrode layer

Using various materials for the electrodes is one option for enhancing SOFC performance. Investigating further advancements in well-proven technologies is another option. An additional catalytic layer placed on the anode side should increase the fuel cell's stability and effectiveness [42]. The impact of specific catalytic layers on SOFC performance, as well as direct internal reforming of biogas, was extensively investigated and compared using the original technique (simultaneous measurements of electrical parameters and analysis of outlet gases from SOFC) [157]. $CeO_{2-\delta}$ doped with transition metals such as Mn, Fe, Co, Ni, and Cu, as well as a non-doped reference material, was constructed and examined. These materials were employed as secondary catalytic layers put on the surface of the SOFC anode to prevent the fuel cell from rapidly degrading because of carbon deposition [157].

The surface contact resistance (ASR) is connected to the surface contact between various units as well as the cell material itself. ASR can only be optimized and decreased to the greatest extent feasible since a specific number of cells and interconnects are necessary for the building of the cell stack.

Nonetheless, it cannot be avoided. The electrode and the contact layer between the electrode and interconnect are the sources of the surface contact resistance on the electrode side. It is possible to ensure enough surface contact between components by improving the contact layer. Moreover, the integrity of the electrical structure can be maintained while the internal and external pressure from the stack is buffered [158].

CGO barrier layers of the highest caliber are essential for low-temperature, high-performance cells. According to Sandoval *et al.* [159], the optimization of the CGO barrier layer in combination with a cutting-edge LSC-based electrode resulted in the cells having an exceptional power density exceeding 1 $W \cdot cm^2$ at 600°C in a typical porous anode-supported YSZ electrolyte cell. Compared to the conventional, high-temperature co-fired barrier layer generated using powder processing, the thick barrier layer created using physical vapor deposition performed significantly better. Frequently, especially for cells operating at low temperatures (600°C), the inclusion of a CGO barrier layer, even a few nanometer thick, eliminates the adverse reactions. Without a barrier layer, a cell displayed strong electrode polarization and a low-power density. In both a commercial and in-house produced cell, powder-processed CGO layers with thicknesses in the range of 5–10 m performed well. They still exhibited a small amount of Sr diffusion to the YSZ, which most likely occurred during the layers' high-temperature sintering (>1000°C). By using the spray-pyrolysis method, alternative, low-temperature processed barrier layers were created. These layers demonstrated significant effectiveness in preventing interdiffusion. For the thinnest tested barrier layer, which was around 300 nm thick, the performance was only marginally worse than the powder-produced layers. Performance was enhanced by the thicker layers, which had thicknesses of 700 and 1500 nm [160].

Because of its low cost, high ionic transference number in oxidizing and reducing atmospheres, and strong chemical and mechanical characteristics, YSZ is the most widely used electrolyte for SOFCs. The YSZ's mechanical qualities enable it to survive operational circumstances as well as residual stresses from cell construction operations. As electrolytes or as a barrier between the YSZ electrolyte and frequently used cathode materials, SDC or GDC can also be used. This prevents the formation of secondary phases with poor conductivity, such as $La_2Zr_2O_7$ or $SrZrO_3$, which can impair cathode performance. It has been demonstrated that using cathode contact layers like $LaNi_{0.6}Fe_{0.4}O_3$ (LNF) and $LaNi_{0.6}Co_{0.4}O_3$ (LNC) improves electron transportation from the interconnect to the cathode layer across the contact interface. The ORR of the TPB in the cathode will also get additional electrons from the interconnector, enhancing the cell's performance [161].

Several studies have recommended the use of buffer/barrier layers between the electrolyte and the electrode layer to minimize chemical interaction at the electrode/electrolyte interface and to avoid diminished electrochemical performance. To date, pure ionic conducting Y, Sm, or Gd-doped ceria-based materials have generally been used as buffer layers in this regard. These purely ionic buffer layers do not actively contribute to improving electrode kinetics via enlargement of the TPB at the electrode/electrolyte interface, despite the fact that these efforts have been shown to be successful in preventing the formation of impurity phases, thereby preventing performance degradation [161].

5. Common fabrication risks

The anode and cathode electrodes cannot be produced or synthesized in a single fabrication step because of the nature of the S-SOFC materials. This section discusses the risks and challenges that are particularly associated with the fabrication method of the complete cell. Basis materials for S-SOFC applications previously studied may react differently depending on the based materials used, including composite materials, anode materials, cathode materials, and even interconnect materials. Original anode materials, for example, were developed to reduce poisoning and coking caused by chromium, sulfur, and even carbon. As cathode and electrolyte-based materials are not optimal for use as anode materials, they may present several difficulties in a reducing environment. Nearly all breakdowns happen at the anode. These materials must be sturdy enough to last while yet without compromising the structure's stability. Consequently, the production process and the operating conditions for the application may both be anticipated when the appropriate materials have been determined. Aside from choosing the appropriate materials, the next paragraph details everything else that must be considered: (1) optimum thickness of the fabricated cell; (2) suitable sintering temperature of the cell; (3) productivity of the fabrication method; (4) cost-effective versus producibility.

Starting with the selection of basic materials and progressing through the synthesis technique, the resulting powders may display noticeably varied particle and microstructure characteristics. For example, the particle size of materials synthesized using GNP is less than that of products synthesized using the sol–gel approach. A detailed inquiry of this topic is required because the following procedure includes cell manufacture. As stated, a desired specific cell with varying thickness is required with an acceptable sintering temperature. The tape casting process is the most acceptable choice in terms of cost-effectiveness and producibility. Tape casting may generate a vast amount of thin, translucent ceramic. However, this approach frequently requires a lengthy ball milling time to prepare the slurry and some slurry may require many milling steps. Furthermore, the irrelevant texture of the post casted tape is attributable to an insufficient formulation. It would be ideal if the sintered tape was a flat ceramic. In most circumstances, if the formulation is incorrect, the ceramic will have a fractured, bent, or wavy texture. Lee *et al.* [36] mentioned a few fabrication difficulties with tape casting in their research. Fig. 7 depicts one of the fabrication difficulties. Additional formulation adjustments and modifications, known as optimizations, are required for the binder

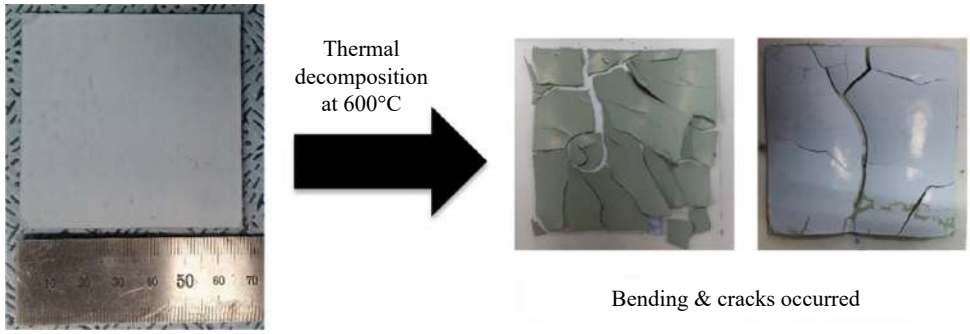

Fig. 7. Example of bending and cracks as reported by Ref. [36] for tape casting. Reprinted from *Int. J. Hydrogen Energy*, 42, S. Lee, K. Lee, Y.H. Jang, and J. Bae, Fabrication of solid oxide fuel cells (SOFCs) by solvent-controlled co-tape casting technique, 1648-1660, Copyright 2017, with permission from Elsevier.

and powder concentration [162].

The screen-printing method offers a simple step fabrication; however, the producibility of this method is of a single film at a time. The thickness and the density of the printed film can be controlled as a matter of the mesh on the screen and the screen printer variable [144]. A common issue with this method is the sintering temperature; that is, in most cases, the printed film is not adhered or sticking well on the substrate. This situation needs to be resolved because the formation of gaps or space between the substrate and the film (delamination) may hinder the performance of the single cell. Considering the high operating temperature of the SOFC application, the component layer needs to undergo good fabrication and heat treatment. Somalu *et al.* [37] reviewed the important parameters for the screen-printing method. Fig. 8 shows various solid contents of the slurry and the resulting properties of the slurry. For the screen-printing method, a few aspects that must be considered are as follows [163]: (1) powder content of slurry (approximately at 70wt%); (b) relative density of powder; (c) slurry homogeneity; (4) screen printer variable parameter (speed, substrate to printer gap size, mesh size).

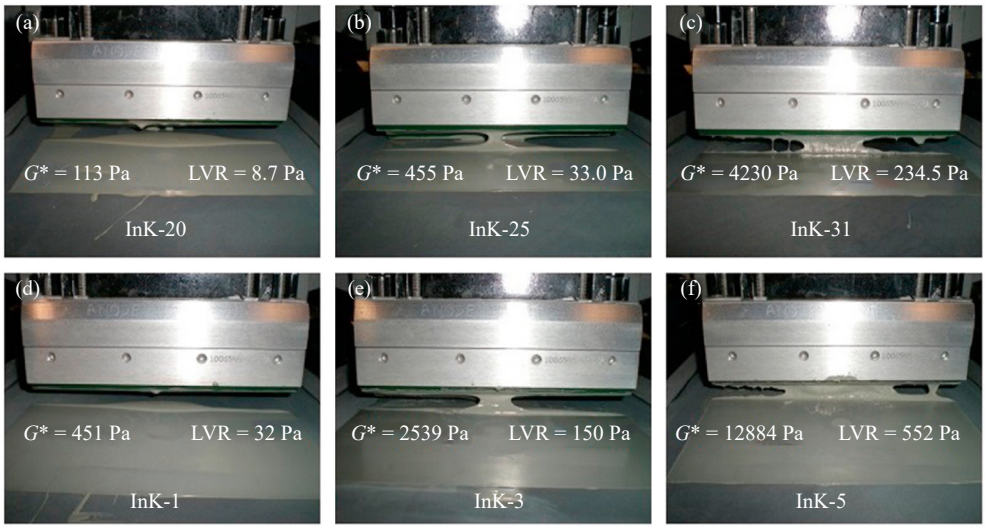

Fig. 8. Effect of various solid contents for screen-printing slurry with variant linear viscoelastic region (LVR) and complex modulus (*G) [37]. Reprinted from *Renew. Sustain. Energy Rev.*, 75, M.R. Somalu, A. Muchtar, W.R.W. Daud, and N.P. Brandon, Screen-printing inks for the fabrication of solid oxide fuel cell films: A review, 426-439, Copyright 2017, with permission from Elsevier.**

Another commonly used fabrication method is spin coating. The spin coating method is considered simple and efficient and consumes less time to fabricate each cell compared with the tape casting method. An electrolyte-supported cell has no issues; however, the same is not true for the electrode (anode or cathode)-supported configuration. The film produced is expected to be thin, and some films can have a porous structure due to the slurry properties [164]. Even though all mentioned methods use slurry as the main aspects, all three slurries differ in terms of powder content, viscosity, and binder used. The method itself can be handy; however, the aspect of preparing the slurry to become suitable and compatible with the process still needs modification and improvement to obtain a durable, stable single cell for the operation [165].

6. Material challenges and perspectives

Most of the material challenges revolve around stability issues. This issue has been reported in conjunction with the great performance of certain materials yet not discussed intensively. This section provides general additional informa-

tion and overview of the challenges in material selection for S-SOFC application from the author perspectives. $La_{0.75}Sr_{0.25}Cr_{0.5}Mn_{0.5}O_{3-\delta}$ (LSCM) has been researched previously. This material possesses a high potential for use as anode and cathode because of its stability in redox cycles and sufficient electrochemical properties, especially for oxidation and reduction reactions [166]. This material records power densities as high as 0.5 and 0.3 $W \cdot cm^{-2}$ at 950°C under H_2 and CH_4 environments, respectively. However, in perovskites, especially manganite, the material stability under reduced environment originating from the insertion of Mn species combined with chromium disintegrates the electroactive species [167–168]. An issue has been reported that gradual decomposition occurs in LSCM tested under a dry diluted hydrogen environment in addition to its endurance under a long-term operation [87].

Considering the appropriate limits of documented power densities in a reduced environment, this material still has potential because the criteria for a material to be used in an S-SOFC are demanding. Furthermore, options are still available for optimizing these materials for slow deterioration when operated in a reduced environment for an extended period. However, material availability for SOFC components is enormously complicated, as each coating must be constructed exclusively with the neighboring components, as well as concerned toward the fuel in materials behavior.

Although cobalt-free-based materials, such as $La_{0.5}Sr_{0.5}Fe_{0.8}Cu_{0.2}O_{3-\delta}$, which were evaluated for R-SOFC by Lu *et al.* [169], exhibited sufficient electrochemical performances, a glitch still occurred. The peak power densities of this S-SOFC configuration achieved as high as 1054 $mW \cdot cm^{-2}$ in H_2 and 894 $mW \cdot cm^{-2}$ in syngas fuel operated at 900°C; these findings can be concluded as the highest among the reported values. For the $La_{0.5}Sr_{0.5}Fe_{0.8}Cu_{0.2}O_{3-\delta}$ electrode, a slight degradation was observed involving current and power density. Performance degradation can be partially due to the nonuniformity of the exsolved Cu particles and the potential time-consuming coarsening of the particles at high temperatures that might decrease the active sites for fuel oxidation reactions. In comparison, the thermal mismatch between the electrodes and the interlayer and the electrolyte can lead to great interface resistance over a long period of time. The same situation was reported by Tian *et al.* [170] when using $La_{0.6}Sr_{0.4}Fe_{0.8}Ni_{0.2}O_{3-\delta}$ as the electrode in R-SFOC. Degradation occurred where a slight aggregation was detected after a medium-term analysis. This phenomenon may result in gas transportation and elevated polarization resistance difficulties. Most perovskite materials that involve the Sr element exhibit Sr segregation easily. This material has outstanding electrochemical performance because of its high-power density.

The Cu and Ni cations were used to improve the stability of these materials when exposed to a reducing environment at a high temperature. Other high catalytic cations, such as Ti, Cr, or Mn, can be added to these materials to increase their catalytic activity. A second consideration is that other factors such as fuel composition and voltage influence the impedance response at high frequencies, whereas combination of proton and oxide ion, as well as the migration of electron/oxide ions and protons influence the impedance response at lower frequencies. Moreover, the smaller microstructure and lower sintering temperature of the anode result in an improvement in the performance of the electrode. Given that both materials exhibit Sr segregation problems, further investigation into the preliminary synthesis technique as well as the microstructure of the materials, particularly because of heat treatment, can provide more information on these problems.

An RP manganite material, $Nd_xAE_{2-x}MnO_{4\pm\delta}$ (AE: Ca, Sr), was developed as a potential electrode for S-SOFC, and the preliminary studies were reported by Sandoval *et al.* [171] $Nd_xSr_{2-x}MnO_{4\pm\delta}$ and $Nd_xACa_{2-x}MnO_{4\pm\delta}$ were synthesized via the sol–gel method and heat treated in air and diluted hydrogen. The single-phase composition was obtained for the two materials heat treated in the air; however, $Nd_xACa_{2-x}MnO_{4\pm\delta}$ was heat treated in a diluted hydrogen environment. $Nd_xCa_{2-x}MnO_{4\pm\delta}$ suffered from decomposition, indicating that this composition is unsuitable to be considered in S-SOFC because of its poor stability. This situation was revealed after XRD analysis, where all the compositions used $Nd_xCa_{2-x}MnO_{4\pm\delta}$ (x = 0.25, 0.4, 0.5, 0.6) into a mixture consisting of Nd_2O_3 and $Ca_{(2-x)/3}MnO_4$ [171].

As discussed earlier, enhancement of materials mostly involves the use of dopant where the element from the transition group is selected because a material with less integration of transition element performs poorly when acting as a cathode than when operated as an anode. The electrochemical performance with low fuel input is relatively poor compared with the known $La_{0.6}Sr_{0.4}Co_{0.2}Fe_{0.8}O_{3-\delta}$ and Ni–YSZ [172]. However, the idea of using a transition element is not always managed to solve the problems because it may experience structure decomposition of perovskites either partially or fully from the anode case, especially when operated in a reducing environment. $Pr_{0.4}Sr_{0.6}Co_{0.2}Fe_{0.7}Nb_{0.1}O_{3-\delta}$ decomposes into K_2NiF_4 structure and Co–Fe alloy [173]; $La_{0.6}Sr_{0.4}Fe_{0.85}Pd_{0.05}Mn_{0.1}O_3$ is partially reduced to K_2NiF_4 structure and metallic Pd [174]. The RP configuration is a completely new sort of configuration in the perovskite's family [175].

The synthesis of the RP material is in and of itself a significant amount of labor because of its complicated structure. Considering that this material works well as an anode yet not as a cathode, it is not a good choice for S-SOFC applications. In oxygen reaction mechanism, a variety of processes can be limiting, depending on the electrode composition, processing parameters, and measurement conditions. However, disagreement continues on the nature of the elementary processes that contribute to polarization resistance in the oxygen reaction mechanism. In summary, this material may have a chance to serve as an electrode for S-SOFCs though only with minor modifications to allow for optimization in all the previously stated aspects. Table 3 summarizes the electrode materials for S-SOFC.

Table 3. List of electrodes for S-SOFC

Ref.	Electrode	Electrolyte	R_p / (Ω·cm^2)		T_O / °C	Power density / (mW·cm^{-2})	Fuel
			Cathode	Anode			
Lanthanum manganite							
[176]	$La_{0.8}Sr_{0.2}MnO_{3-\delta}$–$Gd_{0.2}Ce_{0.8}O_{3-\delta}$	YSZ	1.63	—	800	150.80	Humidified H_2
[86]	$(La_{0.8}Sr_{0.2})_{0.9}Sc_{0.2}Mn_{0.8-x}Ru_xO_{3-\delta}$	Sc_2O_3 stabilized ZrO_2	0.23	0.52	800	318	Wet H_2
Cobalt-free materials							
[177]	$BaFe_{0.9}Zr_{0.1}O_{3-\delta}$ (BFZ)	$La_{0.9}Sr_{0.1}Ga_{0.8}Mg_{0.2}O_{3-\delta}$ (LSGM)	0.105	0.105	800	1097	Humidified H_2
[47]	$SrFe_{0.8}W_{0.2}O_{3-\delta}$	$La_{0.8}Sr_{0.2}Ga_{0.8}Mg_{0.2}O_{3-\delta}$ (LSGM)	0.084	0.20	800	931 (850°C)	H_2
[149]	SDC-$BaZr_{0.1}Co_{0.4}Fe_{0.4}Y_{0.1}O_3$	BZCY	0.32	1.35	700	114.8 (650°C)	H_2–N_2
[39]	$La_{1-x}Sr_xFe_{0.8}Cu_{0.2}O_{3-\delta}$ (x = 0.2, 0.4)	$La_{0.8}Sr_{0.2}Ga_{0.8}Mg_{0.2}O_{3-\delta}$ (LSGM)	0.454	—	800	294	Dry H_2
[43]	$La_{0.5}Sr_{0.5}Fe_{0.9}Mo_{0.1}O_{3-\delta}$	$Sm_{0.2}Ce_{0.8}O_{1.95}$ (SDC)	—	0.083	750	562	H_2/Ar
[43]	$La_{0.5}Sr_{0.5}Fe_{0.9}Mo_{0.1}O_{3-\delta}$	$La_{0.9}Sr_{0.1}Ga_{0.8}Mg_{0.2}O_{3-\delta}$ (LSGM)	—	0.397	750	508	H_2/Ar
[178]	$La_{0.5}Sr_{0.5}Fe_{0.9}W_{0.1}O_{3-\delta}$	$La_{0.8}Sr_{0.2}Ga_{0.8}Mg_{0.2}O_{3-\delta}$	0.08	0.16	800	617.3	Wet H_2
Titanate-based materials							
[33]	$CaTi_{0.6-x}Fe_{0.4}P_xO_{3-\delta}$	YSZ	100.28	70.43	600	58 (800°C)	H_2/Ar
[179]	$La_{0.7}Sr_{0.3}Ti_{0.1}Fe_{0.6}Ni_{0.3}O_{3-\delta}$	LSGM	0.047	0.201	800	—	H_2
[34]	$Sr_2Ti_{0.8}Co_{0.2}FeO_6$	—	0.124	0.380	800	555	H_2
						180	Liquefied petroleum gas
						404	C_2H_5OH
						390	CH_3OH
Ruddlesden–Popper							
[44]	$Sr_2Fe_{1.3}Co_{0.2}Mo_{0.5}O_{6-\delta}$–$Gd_{0.1}Ce_{0.9}O_{2-\delta}$	LSGM	0.036	0.047	800	986	H_2
[180]	$PrNi_{0.4}Fe_{0.6}O_{3-\delta}$	LSGM	—	—	800	663	CH_4
[181]	PrO_x–$Pr_{0.6}Sr_{0.4}FeO_{3-\delta}$	YSZ	0.053	0.113	800	741	Humidified H_2
[182]	Pr–$PrBaMn_2O_{5+\delta}$	YSZ	0.016	0.20	800	423	H_2
[32]	$Sr_2MnMoO_{5+\delta}$/NiO–SDC	SDC	—	0.36	800	245	Wet CH_4
				0.37	800	183	C_2H_5OH

7. Conclusions

This article provides a comprehensive analysis of the development and amazing progress made on electrode materials for use in S-SOFC applications over the past 5 years. As a reference and a guide for future literature studies, we will go through the resource selection process and the issues often cited by those materials. In S-SOFCs, oxygen gas is converted into cathode oxygen ions, which then travel through the dense electrolyte to the porous anode, where it takes part in the electrochemical oxidation of fuel and results in water production. Developing porous electrode materials capable of effectively converting H_2 molecules or hydrocarbon molecules into protons is necessary to make this possible.

Coking on the anode must be avoided whenever possible because hydrocarbon is used as fuel. However, this is often difficult to do with common anode materials, and it is vital to continue monitoring the progression of materials over time. Materials that have been developed recently for use in S-SOFCs highlight the fact that research efforts are picking up speed in terms of the number of studies being conducted. Research efforts on the preliminary properties of materials are still relevant, whether they are newly developed or improved. Additionally, when developing materials, the primary goals of lowering the high operating temperature while maintaining good performance and useful output as well as reducing the amount of labor required, especially during cell fabrication, are the top priorities and can be accomplished. Considering this, it is necessary to offer an overview of recently developed improved materials in addition to performance, focusing specifically on electrochemical presentation.

This works concludes that the practical implementations of S-SOFCs are still far ahead, and a range of issues remains to be overcome. The electrochemical performance and cell durability exceeding the requirement of components are considered significant achievements despite the research coverage compared with conventional SOFC. Numerous research challenges remain to be addressed before a workable, consumer sector becomes feasible, especially regarding the electrode and electrolyte material production. Although existing materials can meet the requirements in terms of electrochemical performance, their long-term stability makes them inadequate for use in new devices. Future experiments must increasingly focus on the long-term reliability of S-SOFCs for the systems to be market ready. The study on electrode materials for S-SOFCs is a substantial research and develop-

ment concern for the global energy market and processing industrial demands. Such material application with proper studies and research will soon become feasible, because global energy consumption is rising because of population expansion, industrialization, and urbanization.

Acknowledgements

The authors acknowledge the Fundamental Research Grant Scheme (FRGS), grant No. FRGS/1/2021/TK0/UKM/01/5 funded by the Ministry of Higher Education (MOHE), Malaysia and Universiti Kebangsaan Malaysia for providing facilities and expertise that greatly assisted this research.

Conflict of Interest

The authors declare that they have no known competing financial interests or personal relationships that could have appeared to influence the work reported in this paper.

References

[1] E. Fabbri, D. Pergolesi, and E. Traversa, Materials challenges toward proton-conducting oxide fuel cells: A critical review, *Chem. Soc. Rev.*, 39(2010), No. 11, p. 4355.

[2] N. Rajalakshmi, R. Balaji, and S. Ramakrishnan, Recent developments in hydrogen fuel cells: Strengths and weaknesses, [in] *Sustainable Fuel Technologies Handbook*, Elsevier, Amsterdam, 2021, p. 431.

[3] X. Fan, M. Tebyetekerwa, Y. Wu, R.R. Gaddam, and X.S. Zhao, Origin of excellent charge storage properties of defective tin disulphide in magnesium/lithium-ion hybrid batteries, *Nano Micro Lett.*, 14(2022), No. 1, art. No. 177.

[4] J.A. Delborne, D. Hasala, A. Wigner, and A. Kinchy, Dueling metaphors, fueling futures: "Bridge fuel" visions of coal and natural gas in the United States, *Energy Res. Soc. Sci.*, 61(2020), art. No. 101350.

[5] Y.J. Yang, Y.H. Yu, J. Li, *et al*., Engineering ruthenium-based electrocatalysts for effective hydrogen evolution reaction, *Nano Micro Lett.*, 13(2021), No. 1, art. No. 160.

[6] Z.W. Cao, R. Momen, S.S. Tao, *et al*., Metal-organic framework materials for electrochemical supercapacitors, *Nano Micro Lett.*, 14(2022), No. 1, art. No. 181.

[7] C. H. Wendel, P. Kazempoor, and R. J. Braun, Novel electrical energy storage system based on reversible solid oxide cells : System design and operating conditions, *J. Power Sources*, 276(2015), p. 133.

[8] X.Y. Huang, L.H. Li, S.F. Zhao, *et al*., MOF-like 3D graphene-based catalytic membrane fabricated by one-step laser scribing for robust water purification and green energy production, *Nano Micro Lett.*, 14(2022), No. 1, art. No. 174.

[9] X.Y. Wang, X.M. Li, H.Q. Fan, and L.T. Ma, Solid electrolyte interface in Zn-based battery systems, *Nano Micro Lett.*, 14(2022), No. 1, art. No. 205.

[10] A. Boudghene Stambouli and E. Traversa, Fuel cells, an alternative to standard sources of energy, *Renew. Sustain. Energy Rev.*, 6(2002), No. 3, p. 295.

[11] T. Wilberforce, A. Alaswad, A. Palumbo, M. Dassisti, and A.G. Olabi, Advances in stationary and portable fuel cell applications, *Int. J. Hydrogen Energy*, 41(2016), No. 37, p. 16509.

[12] H.J. Ying, P.F. Huang, Z. Zhang, *et al*., Freestanding and flexible interfacial layer enables bottom-up Zn deposition toward dendrite-free aqueous Zn-ion batteries, *Nano Micro Lett.*, 14(2022), No. 1, art. No. 180.

[13] B. Zhang, Y.Y. Feng, and W. Feng, Azobenzene-based solar thermal fuels: A review, *Nano Micro Lett*., 14(2022), art. No. 138

[14] J. Romdhane and H. Louahlia-Gualous, Energy assessment of PEMFC based MCCHP with absorption chiller for small scale French residential application, *Int. J. Hydrogen Energy*, 43(2018), No. 42, p. 19661.

[15] S.S.C. Chuang and L. Zhang, Perovskites and related mixed oxides for SOFC applications, [in] *Perovskites and Related Mixed Oxides*, Wiley-VCH Verlag GmbH & Co. KGaA, Weinheim, 2015, p. 863.

[16] G.S. Ma, D. Zhang, P. Guo, *et al*., Phase orientation improved the corrosion resistance and conductivity of Cr_2AlC coatings for metal bipolar plates, *J. Mater. Sci. Technol.*, 105(2022), p. 36.

[17] S.W. Lee, B. Lee, C. Baik, T.Y. Kim, and C. Pak, Multifunctional Ir-Ru alloy catalysts for reversal-tolerant anodes of polymer electrolyte membrane fuel cells, *J. Mater. Sci. Technol.*, 60(2021), p. 105.

[18] H.A. Tahini, X. Tan, W. Zhou, Z.H. Zhu, U. Schwingenschlögl, and S.C. Smith, Sc and Nb dopants in $SrCoO_3$ modulate electronic and vacancy structures for improved water splitting and SOFC cathodes, *Energy Storage Mater.*, 9(2017), p. 229.

[19] R. Pelosato, G. Cordaro, D. Stucchi, C. Cristiani, and G. Dotelli, Cobalt based layered perovskites as cathode material for intermediate temperature Solid Oxide Fuel Cells: A brief review, *J. Power Sources*, 298(2015), p. 46.

[20] A. Choudhury, H. Chandra, and A. Arora, Application of solid oxide fuel cell technology for power generation—A review, *Renew. Sustain. Energy Rev.*, 20(2013), p. 430.

[21] H.B. Li, N. Xu, Y.H. Fang, H. Fan, Z. Lei, and M.F. Han, Syngas production via coal char-CO_2 fluidized bed gasification and the effect on the performance of LSCFN// LSGM// LSCFN solid oxide fuel cell, *J. Mater. Sci. Technol.*, 34(2018), No. 2, p. 403.

[22] Y.P. Wang, S.H. Liu, H.Y. Zhang, *et al*., Structured $La_{0.6}Sr_{0.4}Co_{0.2}Fe_{0.8}O_{3-\delta}$ cathode with large-scale vertical cracks by atmospheric laminar plasma spraying for IT-SOFCs, *J. Alloys Compd.*, 825(2020), art. No. 153865.

[23] M. Mogensen and K. Kammer, Conversion of hydrocarbons in solid oxide fuel cells, *Annu. Rev. Mater. Res.*, 33(2003), No. 1, p. 321.

[24] M.D. Fernandes, V. Bistritzki, R.Z. Domingues, T. Matencio, M. Rapini, and R.D. Sinisterra, Solid oxide fuel cell technology paths: National innovation system contributions from Japan and the United States, *Renew. Sustain. Energy Rev.*, 127(2020), p. 109879.

[25] K. Huang and S.C. Singhal, Cathode-supported tubular solid oxide fuel cell technology: A critical review, *J. Power Sources*, 237(2013), p. 84.

[26] M.S. Javed, N. Shaheen, A. Idrees, C.G. Hu, and R. Raza, Electrochemical investigations of cobalt-free perovskite cathode material for intermediate temperature solid oxide fuel cell, *Int. J. Hydrogen Energy*, 42(2017), No. 15, p. 10416.

[27] V. Sarıboğa and M.A. Faruk Öksüzömer, Cu−CeO_2 anodes for solid oxide fuel cells: Determination of infiltration characteristics, *J. Alloys Compd.*, 688(2016), p. 323.

[28] H. Aslannejad, L. Barelli, A. Babaie, and S. Bozorgmehri, Effect of air addition to methane on performance stability and coking over NiO−YSZ anodes of SOFC, *Appl. Energy*, 177(2016), p. 179.

[29] W.X. Kao, M.C. Lee, Y.C. Chang, T.N. Lin, C.H. Wang, and J.C. Chang, Fabrication and evaluation of the electrochemical

performance of the anode-supported solid oxide fuel cell with the composite cathode of $La_{0.8}Sr_{0.2}MnO_{3-\delta}$-Gadolinia-doped ceria oxide/$La_{0.8}Sr_{0.2}MnO_{3-\delta}$, *J. Power Sources*, 195(2010), No. 19, p. 6468.

[30] A.A. Jais, S.A. Ali, M. Anwar, *et al*., Performance of Ni/10Sc_1CeSZ anode synthesized by glycine nitrate process assisted by microwave heating in a solid oxide fuel cell fueled with hydrogen or methane, *J. Solid State Electrochem.*, 24(2020), p. 711.

[31] K. Venkataramana, C. Madhuri, C. Madhusudan, Y.S. Reddy, G. Bhikshamaiah, and C.V. Reddy, Investigation on La^{3+} and Dy^{3+} co-doped ceria ceramics with an optimized average atomic number of dopants for electrolytes in IT-SOFCs, *Ceram. Int.*, 44(2018), No. 6, p. 6300.

[32] X.Z. Peng, Y.F. Tian, Y. Liu, *et al*., A double perovskite decorated carbon-tolerant redox electrode for symmetrical SOFC, *Int. J. Hydrogen Energy*, 45(2020), No. 28, p. 14461.

[33] L. dos Santos-Gómez, J.M. Porras-Vázquez, E.R. Losilla, D. Marrero-López, and P.R. Slater, Investigation of PO_4^{3-} oxyanion-doping on the properties of $CaFe_{0.4}Ti_{0.6}O_{3-\delta}$ for potential application as symmetrical electrodes for SOFCs, *J. Alloys Compd.*, 835(2020), art. No. 155437.

[34] B.B. Niu, C.L. Lu, W.D. Yi, *et al.*, *In-situ* growth of nanoparticles-decorated double perovskite electrode materials for symmetrical solid oxide cells, *Appl. Catal., B*, 270(2020), art. No. 118842.

[35] W.W. Fan, Z. Sun, Y. Bai, K. Wu, and Y.H. Cheng, Highly stable and efficient perovskite ferrite electrode for symmetrical solid oxide fuel cells, *ACS Appl. Mater. Interfaces*, 11(2019), No. 26, p. 23168.

[36] S.H. Lee, K. Lee, Y.H. Jang, and J. Bae, Fabrication of solid oxide fuel cells (SOFCs) by solvent-controlled co-tape casting technique, *Int. J. Hydrogen Energy*, 42(2017), No. 3, p. 1648.

[37] M.R. Somalu, A. Muchtar, W.R.W. Daud, and N.P. Brandon, Screen-printing inks for the fabrication of solid oxide fuel cell films: A review, *Renew. Sustain. Energy Rev.*, 75(2017), p. 426.

[38] L. Bernadet, C. Moncasi, M. Torrell, and A. Tarancón, High-performing electrolyte-supported symmetrical solid oxide electrolysis cells operating under steam electrolysis and co-electrolysis modes, *Int. J. Hydrogen Energy*, 45(2020), No. 28, p. 14208.

[39] F. Zurlo, I. Natali Sora, V. Felice, *et al*., Copper-doped lanthanum ferrites for symmetric SOFCs, *Acta Mater.*, 112(2016), p. 77.

[40] J. C. Ruiz-Morales, D. Marrero-López, J. Canales-Vázquez, and J. T. S. Irvine, Symmetric and reversible solid oxide fuel cells, *RSC Adv.*, 1(2011), No. 8, p. 1403.

[41] C. Su, W. Wang, M. Liu, M. O. Tadé, and Z. Shao, Progress and Prospects in Symmetrical Solid Oxide Fuel Cells with Two Identical Electrodes, *Adv. Energy Mater.*, 5(2015), No. 14, p. 1500188.

[42] X. Chen, J.T. Wang, N. Yu, *et al*., A robust direct-propane solid oxide fuel cell with hierarchically oriented full ceramic anode consisting with in-situ exsolved metallic nano-catalysts, *J. Membr. Sci.*, 677(2023), art. No. 121637.

[43] H.D. Cai, L.L. Zhang, J.S. Xu, *et al*., Cobalt-free $La_{0.5}Sr_{0.5}Fe_{0.9}Mo_{0.1}O_{3-\delta}$ electrode for symmetrical SOFC running on H_2 and CO fuels, *Electrochim. Acta*, 320(2019), art. No. 134642.

[44] Y.R. Yang, S.S. Li, Z.B. Yang, *et al*., One step synthesis of $Sr_2Fe_{1.3}Co_{0.2}Mo_{0.5}O_{6-\delta}$-$Gd_{0.1}Ce_{0.9}O_{2-\delta}$ for symmetrical solid oxide fuel cells, *J. Electrochem. Soc.*, 167(2020), No. 8, art. No. 084503.

[45] Y.Z. Lu, N. Mushtaq, M.A.K. Yousaf Shah, *et al*., $Ba_{0.5}Sr_{0.5}Fe_{0.8}Sb_{0.2}O_{3-\delta}$-$m_{0.2}Ce_{0.8}O_{2-\delta}$ bulk heterostructure composite: A cobalt free Oxygen Reduction Electrocatalyst for low-temperature SOFCs, *Int. J. Hydrogen Energy*, 47(2022), No. 90, p. 38348.

[46] Y.Z. Lu, J.J. Li, L.G. Ma, Z.H. Lu, L. Yu, and Y.X. Cai, The development of semiconductor-ionic conductor composite electrolytes for fuel cells with symmetrical electrodes, *Int. J. Hydrogen Energy*, 46(2021), No. 15, p. 9835.

[47] Y.X. Cao, Z.W. Zhu, Y.J. Zhao, W. Zhao, Z.L. Wei, and T. Liu, Development of tungsten stabilized $SrFe_{0.8}W_{0.2}O_{3-\delta}$ material as novel symmetrical electrode for solid oxide fuel cells, *J. Power Sources*, 455(2020), art. No. 227951.

[48] H.Z. Lv, Q. Pan, Y. Song, X.X. Liu, and T.Y. Liu, A review on nano-/microstructured materials constructed by electrochemical technologies for supercapacitors, *Nano Micro Lett.*, 12(2020), No. 1, p. 1.

[49] J.V. Reis, T.C.P. Pereira, T.H.A. Teles, *et al*., Synthesis of $CeNb_3O_9$ perovskite by pechini method, *Mater. Lett.*, 227(2018), p. 261.

[50] Y.X. Chen, S.L. Luo, J. Leng, *et al*., Exploring the synthesis conditions and formation mechanisms of Li-rich layered oxides via solid-state method, *J. Alloys Compd.*, 854(2021), art. No. 157204.

[51] S.Q. Zhao, Z.Q. Guo, K. Yan, *et al*., Towards high-energy-density lithium-ion batteries: Strategies for developing high-capacity lithium-rich cathode materials, *Energy Storage Mater.*, 34(2021), p. 716.

[52] Y.L. Gao, Z.H. Pan, J.G. Sun, Z.L. Liu, and J. Wang, High-energy batteries: Beyond lithium-ion and their long road to commercialisation, *Nanomicro Lett.*, 14(2022), No. 1, art. No. 94.

[53] B. Zhu, R. Raza, H.Y. Qin, and L.D. Fan, Single-component and three-component fuel cells, *J. Power Sources*, 196(2011), No. 15, p. 6362.

[54] H.Q. Hu, Q.Z. Lin, Z.G. Zhu, B. Zhu, and X.R. Liu, Fabrication of electrolyte-free fuel cell with $Mg_{0.4}Zn_{0.6}O$/$Ce_{0.8}Sm_{0.2}O_{2-\delta}$-$Li_{0.3}Ni_{0.6}Cu_{0.07}Sr_{0.03}O_{2-\delta}$ layer, *J. Power Sources*, 248(2014), p. 577.

[55] K. Lin, X.F. Xu, X.Y. Qin, *et al.*, Commercially viable hybrid Li-ion/metal batteries with high energy density realized by symbiotic anode and prelithiated cathode, *Nano Micro Lett.*, 14(2022), art. No. 149.

[56] P. Mukherjee, N.V. Faenza, N. Pereira, *et al*., Surface structural and chemical evolution of layered $LiNi_{0.8}Co_{0.15}Al_{0.05}O_2$ (NCA) under high voltage and elevated temperature conditions, *Chem. Mater.*, 30(2018), No. 23, p. 8431.

[57] T.P. Gao, K.W. Wong, and K.M. Ng, High-quality $LiNi_{0.8}Co_{0.15}Al_{0.05}O_2$ cathode with excellent structural stability: Suppressed structural degradation and pore defects generation, *Nano Energy*, 73(2020), p. 104798.

[58] Y. Makimura, S.J. Zheng, Y. Ikuhara, and Y. Ukyo, Microstructural observation of $LiNi_{0.8}Co_{0.15}Al_{0.05}O_2$ after charge and discharge by scanning transmission electron microscopy, *J. Electrochem. Soc.*, 159(2012), No. 7, p. A1070.

[59] A.S. Bagishev, D.V. Maslennikov, M.P. Popov, and A.P. Nemudry, A study of the influence of Li-containing additives in microtubular SOFC components based on Gd-doped ceria on the effectiveness of the co-firing method, *Mater. Today*, 25(2020), p. 464.

[60] J.J. Xu, Critical review on cathode-electrolyte interphase toward high-voltage cathodes for Li-ion batteries, *Nano Micro Lett.*, 14(2022), art. No. 166

[61] M.H. Yuan, W.J. Dong, L.L. Wei, *et al*., Stability study of SOFC using layered perovskite oxide $La_{1.85}Sr_{0.15}CuO_4$ mixed with ionic conductor as membrane, *Electrochim. Acta*, 332(2020), art. No. 135487.

[62] E. Thauer, G.S. Zakharova, S.A. Wegener, Q. Zhu, and R. Klingeler, Sol−gel synthesis of Li_3VO_4/C composites as anode materials for lithium-ion batteries, *J. Alloys Compd.*, 853(2021), art. No. 157364.

[63] Y.X. Jiang, L.Y. Chai, D.H. Zhang, *et al*., Facet-controlled $LiMn_2O_4$/C as deionization electrode with enhanced stability and high desalination performance, *Nano Micro Lett.*, 14(2022), No. 1, art. No. 176.

[64] D.L. Ma, Z.Y. Cao, and A.M. Hu, Si-based anode materials for Li-ion batteries: A mini review, *Nano Micro Lett.*, 6(2014), No. 4, p. 347.

[65] A. U. Rehman, M.R. Li, R. Knibbe, M.S. Khan, W. Zhou, and Z.H. Zhu, Unveiling lithium roles in cobalt-free cathodes for efficient oxygen reduction reaction below 600°C, *ChemElectroChem*, 6(2019), No. 20, p. 5340.

[66] X.B. Zhang, G. Chen, Y. He, L.L. Zhang, D. Yang, and S.J. Geng, Effect of Li_2CO_3 and LiOH on the ionic conductivity of $BaCe_{0.9}Y_{0.1}O_3$ electrolyte in SOFCs with a lithium compound electrode, *Int. J. Hydrogen Energy*, 46(2021), No. 15, p. 9948.

[67] Y. He, G. Chen, X.B. Zhang, *et al*., Mechanism for major improvement in SOFC electrolyte conductivity when using lithium compounds as anode, *ACS Appl. Energy Mater.*, 3(2020), No. 5, p. 4134.

[68] L.D. Fan and P.C. Su, Layer-structured $LiNi_{0.8}Co_{0.2}O_2$: A new triple ($H^+/O^{2-}/e^-$) conducting cathode for low temperature proton conducting solid oxide fuel cells, *J. Power Sources*, 306(2016), p. 369.

[69] W.Y. Tan, L.D. Fan, R. Raza, M.A. Khan, and B. Zhu, Studies of modified lithiated NiO cathode for low temperature solid oxide fuel cell with ceria-carbonate composite electrolyte, *Int. J. Hydrogen Energy*, 38(2013), No. 1, p. 370.

[70] G. Chen, H.L. Liu, Y. He, *et al*., Electrochemical mechanisms of an advanced low-temperature fuel cell with a $SrTiO_3$ electrolyte, *J. Mater. Chem. A*, 7(2019), No. 16, p. 9638.

[71] W.W. Fan, Z. Sun, J.K. Wang, J. Zhou, K. Wu, and Y.H. Cheng, Evaluation of $Sm_{0.95}Ba_{0.05}Fe_{0.95}Ru_{0.05}O_3$ as a potential cathode material for solid oxide fuel cells, *RSC Adv.*, 6(2016), No. 41, p. 34564.

[72] C.G. Moura, J.P. de F. Grilo, D.A. Macedo, M.R. Cesário, D.P. Fagg, and R.M. Nascimento, Cobalt-free perovskite $Pr_{0.5}Sr_{0.5}Fe_{1-x}Cu_xO_{3-\delta}$ (PSFC) as a cathode material for intermediate temperature solid oxide fuel cells, *Mater. Chem. Phys.*, 180(2016), p. 256.

[73] X.B. Huang, J. Feng, H.R.S. Abdellatif, J. Zou, G. Zhang, and C.S. Ni, Electrochemical evaluation of double perovskite $PrBaCo_{2-x}Mn_xO_{5+\delta}$ (x = 0, 0.5, 1) as promising cathodes for IT-SOFCs, *Int. J. Hydrogen Energy*, 43(2018), No. 18, p. 8962.

[74] Y.B. He, F. Ning, Q.H. Yang, *et al*., Structural and thermal stabilities of layered $Li(Ni_{1/3}Co_{1/3}Mn_{1/3})O_2$ materials in 18650 high power batteries, *J. Power Sources*, 196(2011), No. 23, p. 10322.

[75] X.Q. Liu, W.J. Dong, Y.Z. Tong, *et al*., Li effects on layer-structured oxide $Li_xNi_{0.8}Co_{0.15}Al_{0.05}O_{2-\delta}$: Improving cell performance via on-line reaction, *Electrochim. Acta*, 295(2019), p. 325.

[76] K. Wang, D. Zheng, H.D. Cai, *et al*., Rational design of favourite lithium-ion cathode materials as electrodes for symmetrical solid oxide fuel cells, *Ceram. Int.*, 47(2021), No. 21, p. 30536.

[77] G.L. Wang, J.Z. Wu, S. Li, *et al*., Effect of the online reaction byproducts of $LiNi_{0.8}Co_{0.15}Al_{0.05}O_{2-\delta}$ electrodes on the performance of solid oxide fuel cells, *Int. J. Hydrogen Energy*, 47(2022), No. 79, p. 33850.

[78] X.F. Luo, X.Y. Wang, L. Liao, X.M. Wang, S. Gamboa, and P.J. Sebastian, Effects of synthesis conditions on the structural and electrochemical properties of layered $Li[Ni_{1/3}Co_{1/3}Mn_{1/3}]O_2$ cathode material via the hydroxide co-precipitation method LIB SCITECH, *J. Power Sources*, 161(2006), No. 1, p. 601.

[79] E.Y. Hu, Z. Jiang, L.D. Fan, *et al*., Junction and energy band on novel semiconductor-based fuel cells, *iScience*, 24(2021), No. 3, p. 102191.

[80] S.M. Baba, N. Ohguri, Y. Suzuki, and K. Murakami, Evaluation of a variable flow ejector for anode gas circulation in a 50-kW class SOFC, *Int. J. Hydrogen Energy*, 45(2020), No. 19, p. 11297.

[81] P. Li, Q.Y. Yang, H. Zhang, M.X. Yao, F. Yan, and D. Fu, Effect of Fe, Ni and Zn dopants in $La_{0.9}Sr_{0.1}CoO_3$ on the electrochemical performance of single-component solid oxide fuel cell, *Int. J. Hydrogen Energy*, 45(2020), No. 20, p. 11802.

[82] D. Zheng, X.M. Zhou, Z.L. He, *et al*., LiNi-oxide simultaneously as electrolyte and symmetrical electrode for low-temperature solid oxide fuel cell, *Int. J. Hydrogen Energy*, 47(2022), No. 63, p. 27177.

[83] M.V. Sandoval, C. Cárdenas, E. Capoen, C. Pirovano, P. Roussel, and G.H. Gauthier, Performance of $La_{0.5}Sr_{1.5}MnO_{4\pm\delta}$ Ruddlesden−Popper manganite as electrode material for symmetrical solid oxide fuel cells. Part A. The oxygen reduction reaction, *Electrochim. Acta*, 304(2019), p. 415.

[84] G. Chen, Y. Gao, Y.F. Luo, and R.F. Guo, Effect of A site deficiency of LSM cathode on the electrochemical performance of SOFCs with stabilized zirconia electrolyte, *Ceram. Int.*, 43(2017), No. 1, p. 1304.

[85] J.K. Wang, J. Zhou, J.M. Yang, *et al*., Nanoscale architecture of $(La_{0.6}Sr_{1.4})_{0.95}Mn_{0.9}B_{0.1}O_4$ (B=Co, Ni, Cu) Ruddlesden−Popper oxides as efficient and durable catalysts for symmetrical solid oxide fuel cells, *Renew. Energy*, 157(2020), p. 840.

[86] J. Zhou, N. Wang, J.J. Cui, *et al*., Structural and electrochemical properties of *B*-site Ru-doped $(La_{0.8}Sr_{0.2})_{0.9}Sc_{0.2}Mn_{0.8}O_{3-\delta}$ as symmetrical electrodes for reversible solid oxide cells, *J. Alloys Compd.*, 792(2019), p. 1132.

[87] S. Durán, N. Rangel, C. Silva, *et al*., Study of $La_4BaCu_{5-x}M_nxO_{13+\delta}$ materials as potential electrode for symmetrical-SOFC, *Solid State Ionics*, 341(2019), p. 115031.

[88] W. Yusoff, N.W. Norman, A. Samat, M.R. Somalu, A. Muchtar, and N.A. Baharuddin, Fabrication process of cathode materials for solid oxide fuel cells, *J. Adv. Res. Fluid Mech. Therm. Sci.*, 2(2018), No. 2, p. 153.

[89] S. Paydar, M.H. Shariat, and S. Javadpour, Investigation on electrical conductivity of LSM/YSZ8, LSM/$Ce_{0.84}Y_{0.16}O_{0.96}$ and LSM/$Ce_{0.42}Zr_{0.42}Y_{0.16}O_{0.96}$ composite cathodes of SOFCs, *Int. J. Hydrogen Energy*, 41(2016), No. 48, p. 23145.

[90] A. Kudryavtsev, S. Lavrov, A. Shestakova, L. Kulyuk, and E. Mishina, Second harmonic generation in nanoscale films of transition metal dichalcogenide: Accounting for multipath interference, *AIP Adv.*, 6(2016), art. No. 095306.

[91] L. Suescun, B. Dabrowski, J. Mais, *et al*., Oxygen ordered phases in $La_xSr_{1-x}MnO_y$ ($0\leq x\leq 0.2$, $2.5\leq y\leq 3$): An *in situ* neutron powder diffraction study, *Chem. Mater.*, 20(2008), No. 4, p. 1636.

[92] M.V. Sandoval, C. Pirovano, E. Capoen, *et al.*, In-depth study of the Ruddlesden-Popper $La_xSr_{2-x}MnO_{3-\delta}$ family as possible electrode materials for symmetrical SOFC, *Int. J. Hydrogen Energy*, 42(2017), No. 34, art. No. 21930.

[93] M. Al Daroukh, V.V. Vashook, H. Ullmann, F. Tietz, and I. Arual Raj, Oxides of the AMO_3 and A_2MO_4-type: Structural stability, electrical conductivity and thermal expansion, *Solid State Ionics*, 158(2003), No. 1-2, p. 141.

[94] E. Lay, G. Gauthier, and L. Dessemond, Preliminary studies of the new Ce-doped La/Sr chromo-manganite series as potential SOFC anode or SOEC cathode materials, *Solid State Ionics*, 189(2011), No. 1, p. 91.

[95] E. Gager, M. Frye, D.C. McCord, J. Scheffe, and J. Nino, Reticulated porous lanthanum strontium manganite structures for solar thermochemical hydrogen production, *Int. J. Hydrogen Energy*, 47(2022), No. 73, p. 31152.

[96] Z.K. Zhu, M. Sugimoto, U. Pal, S. Gopalan, and S. Basu, Mul-

tiple cycle chromium poisoning and *in-situ* electrochemical cleaning of LSM-based solid oxide fuel cell cathodes, *J. Power Sources Adv.*, 6(2020), art. No. 100037.

[97] D. Garcés, A.L. Soldati, H. Troiani, A. Montenegro-Hernández, A. Caneiro, and L.V. Mogni, La/Ba-based cobaltites as IT-SOFC cathodes: A discussion about the effect of crystal structure and microstructure on the O_2-reduction reaction, *Electrochim. Acta*, 215(2016), p. 637.

[98] J.S. Hardy, C.A. Coyle, J.F. Bonnett, *et al.*, Evaluation of cation migration in lanthanum strontium cobalt ferrite solid oxide fuel cell cathodes via in-operando X-ray diffraction, *J. Mater. Chem. A*, 6(2018), No. 4, p. 1787.

[99] N.A. Baharuddin, A. Muchtar, M.R. Somalu, and A.A. Samat, Thermal decomposition of cobalt free $SrFe_{0.9}Ti_{0.1}O_{3+\delta}$ cathode for intermediate temperature solid oxide fuel cell, *Procedia Eng.*, 148(2016), p. 72.

[100] F.F. Dong, Y.B. Chen, D.J. Chen, and Z.P. Shao, Surprisingly high activity for oxygen reduction reaction of selected oxides lacking long oxygen-ion diffusion paths at intermediate temperatures: A case study of cobalt-free $BaFeO_{3-\delta}$, *ACS Appl. Mater. Interfaces*, 6(2014), No. 14, p. 11180.

[101] G.M. Yang, J. Shen, Y.B. Chen, M.O. Tadé, and Z.P. Shao, Cobalt-free $Ba_{0.5}Sr_{0.5}Fe_{0.8}Cu_{0.1}Ti_{0.1}O_{3-\delta}$ as a bi-functional electrode material for solid oxide fuel cells, *J. Power Sources*, 298(2015), p. 184.

[102] W. Jung and H.L. Tuller, A new model describing solid oxide fuel cell cathode kinetics: Model thin film $SrTi_{1-x}Fe_xO_{3-\delta}$ mixed conducting oxides-A case study, *Adv. Energy Mater.*, 1(2011), No. 6, p. 1184.

[103] J. Zamudio-García, L. dos Santos-Gómez, J.M. Porras-Vázquez, E.R. Losilla, and D. Marrero-López, Symmetrical solid oxide fuel cells based on titanate nanocomposite electrodes, *J. Eur. Ceram. Soc.*, 43(2023), No. 4, p. 1548.

[104] X. Chen, C.C. Kou, X.J. Liao, *et al.*, Plasma-sprayed lanthanum-doped strontium titanate as an interconnect for solid oxide fuel cells: Effects of powder size and process conditions, *J. Alloys Compd.*, 876(2021), art. No. 160212.

[105] H. Miao, B. Chen, X. Wu, Q. Wang, P. Lin, J. Wang, C. Yang, H. Zhang, and J. Yuan, Optimizing strontium titanate anode in solid oxide fuel cells by ytterbium doping, *Int. J. Hydrogen Energy*, 44(2019), No. 26, p. 13728.

[106] R.P. Li, C. Zhang, J.H. Liu, J.W. Zhou, and L. Xu, A review on the electrical properties of doped $SrTiO_3$ as anode materials for solid oxide fuel cells, *Mater. Res. Express*, 6(2019), No. 10, art. No. 102006.

[107] D. Dogu, S. Gunduz, K.E. Meyer, D.J. Deka, A.C. Co, and U.S. Ozkan, CO_2 and H_2O electrolysis using solid oxide electrolyzer cell (SOEC) with La and Cl-doped strontium titanate cathode, *Catal. Lett.*, 149(2019), No. 7, p. 1743.

[108] M.A. Yatoo and S.J. Skinner, Ruddlesden-Popper phase materials for solid oxide fuel cell cathodes: A short review, *Mater. Today*, 56(2022), p. 3747.

[109] A. Ndubuisi, S. Abouali, K. Singh, and V. Thangadurai, Recent advances, practical challenges, and perspectives of intermediate temperature solid oxide fuel cell cathodes, *J. Mater. Chem. A*, 10(2022), No. 5, p. 2196.

[110] Z.Y. Han, J.H. Bai, X. Chen, X.F. Zhu, and D.F. Zhou, Novel cobalt-free $Pr_2Ni_{1-x}Nb_xO_4$ (x = 0, 0.05, 0.10, and 0.15) perovskite as the cathode material for IT-SOFC, *Int. J. Hydrogen Energy*, 46(2021), No. 21, p. 11894.

[111] N. Wu, W. Wang, Y.J. Zhong, G.M. Yang, J.F. Qu, and Z.P. Shao, Nickel-iron alloy nanoparticle-decorated K_2NiF_4-type oxide as an efficient and sulfur-tolerant anode for solid oxide fuel cells, *ChemElectroChem*, 4(2017), No. 9, p. 2378.

[112] Z.Q. Xu, Y.H. Li, Y.H. Wan, S.W. Zhang, and C.R. Xia, Nickel enriched Ruddlesden-Popper type lanthanum strontium manganite as electrode for symmetrical solid oxide fuel cell, *J. Power Sources*, 425(2019), p. 153.

[113] S.J. Zhou, Y. Yang, H. Chen, and Y.H. Ling, *in situ* exsolved Co−Fe nanoparticles on the Ruddlesden−Popper-type symmetric electrodes for intermediate temperature solid oxide fuel cells, *Ceram. Int.*, 46(2020), No. 11, p. 18331.

[114] L. Fu, J. Zhou, J. Yang, Z. Lian, J. Wang, Y. Cheng, and K. Wu., Exsolution of Cu nanoparticles in $(LaSr)_{0.9}Fe_{0.9}Cu_{0.1}O_4$ Ruddlesden–Popper oxide as symmetrical electrode for solid oxide cells, *Appl. Surf. Sci.*, 511(2020), p. 145525.

[115] Y. Wang, X.C. Tang, S. Cao, X. Fang, Z.H. Rong, and X. Chen, A novel method to synthesis titanium dioxide(B)/Anatase composite oxides by solid-state chemical reaction routes for promoting Li^+ insertion, *Results Phys.*, 14(2019), art. No. 102451.

[116] O.L. Pineda, Z.L. Moreno, P. Roussel, K. Świerczek, and G.H. Gauthier, Synthesis and preliminary study of the double perovskite $NdBaMn_2O_{5+\delta}$ as symmetric SOFC electrode material, *Solid State Ionics*, 288(2016), p. 61.

[117] N. Li, Z. Lü, B. Wei, *et al.*, Characterization of $GdBaCo_2O_{5+\delta}$ cathode for IT-SOFCs, *J. Alloys Compd.*, 454(2008), No. 1-2, p. 274.

[118] D.J. Chen, R. Ran, K. Zhang, J. Wang, and Z.P. Shao, Intermediate-temperature electrochemical performance of a polycrystalline $PrBaCo_2O_{5+\delta}$ cathode on samarium-doped ceria electrolyte, *J. Power Sources*, 188(2009), No. 1, p. 96.

[119] G. Kim, S. Wang, A.J. Jacobson, L. Reimus, P. Brodersen, and C.A. Mims, Rapid oxygen ion diffusion and surface exchange kinetics in $PrBaCo_2O_{5+x}$ with a perovskite related structure and ordered A cations, *J. Mater. Chem.*, 17(2007), No. 24, p. 2500.

[120] I.A. Ditenberg, I.V. Smirnov, K.V. Grinyaev, D.A. Osipov, A.I. Gavrilov, and M.A. Korchagin, Morphology, structural-phase state and microhardness of a multicomponent non-equiatomic W−Ta−Mo−Nb−Zr−Cr−Ti powders mixture depending on the duration of ball milling, *Adv. Powder Technol.*, 31(2020), No. 10, p. 4401.

[121] A.V. Syugaev, K.A. Yazovskikh, A.A. Shakov, S.F. Lomayeva, and A.N. Maratkanova, Molecular transformations in interfaces and liquid media under wet ball milling of iron with *N*-phenylanthranilic acid, *Colloids Surf. A*, 608(2021), art. No. 125620.

[122] H.B. Li, J. He, Q.Q. Sun, and S. Wang, Effect of the environment on the morphology of Ni powder during high-energy ball milling, *Mater. Today Commun.*, 25(2020), art. No. 101288.

[123] K. Ponhan, K. Tassenberg, D. Weston, K.G.M. Nicholls, and R. Thornton, Effect of SiC nanoparticle content and milling time on the microstructural characteristics and properties of Mg−SiC nanocomposites synthesized with powder metallurgy incorporating high-energy ball milling, *Ceram. Int.*, 46(2020), No. 17, p. 26956.

[124] M.Y. Gong, C.L. Liu, J. Gao, A.Z. Du, W.P. Tong, and C.Z. Liu, Magnetic and electromagnetic properties of $Fe/Fe_{2-3}N$ composites prepared by high-energy ball milling, *J. Mater. Res. Technol.*, 9(2020), No. 4, p. 8646.

[125] P. Sivakumar, R. Ishak, and V. Tricoli, Novel Pt–Ru nanoparticles formed by vapour deposition as efficient electrocatalyst for methanol oxidation: Part I. Preparation and physical characterization, *Electrochim. Acta*, 50(2005), No. 16-17, p. 3312.

[126] T. L. Simonenko, N. P. Simonenko, A. S. Mokrushin, *et al.*, Microstructural, electrophysical and gas-sensing properties of CeO_2–Y_2O_3 thin films obtained by the sol−gel process, *Ceram. Int.*, 46(2020), No. 1, p. 121.

[127] H. Laysandra, D. Triyono, H.L. Liu, and R.A. Rafsanjani, Systematic study of phase-formation and lattice structure of $La_{0.9}Sr_{0.1}Fe_{1-x}Mo_xO_3$ synthesized through the sol−gel method, *Ceram. Int.*, 46(2020), No. 7, p. 9751.

[128] A.A. Samat, W.N.A. Wan Yusoff, N.W. Norman, M.R. Somalu, and N. Osman, Powder and electrical properties of $La_{0.6}Sr_{0.4}CoO_{3-\delta}$ cathode material prepared by a modified sol–gel method for solid oxide fuel cell application, *Jurnal Kejuruteraan*, 1(2018), No. 2, p. 49.

[129] S.K. Badge and A.V. Deshpande, Study of dielectric and ferroelectric properties of Bismuth Titanate ($Bi_4Ti_3O_{12}$) ceramic prepared by sol–gel synthesis and solid state reaction method with varying sintering temperature, *Solid State Ionics*, 334(2019), p. 21.

[130] D. Mateos, B. Valdez, J.R. Castillo, *et al.*, Synthesis of high purity nickel oxide by a modified sol-gel method, *Ceram. Int.*, 45(2019), No. 9, p. 11403.

[131] E.M. Modan and A.G. Plăiaşu, Advantages and disadvantages of chemical methods in the elaboration of nanomaterials, *Ann. "Dunarea De Jos" Univ. Galati Fascicle IX Metall. Mater. Sci.*, 43(2020), No. 1, p. 53.

[132] P.G. Jamkhande, N.W. Ghule, A.H. Bamer, and M.G. Kalaskar, Metal nanoparticles synthesis: An overview on methods of preparation, advantages and disadvantages, and applications, *J. Drug Deliv. Sci. Technol.*, 53(2019), art. No. 101174.

[133] N.A. Baharuddin, A. Muchtar, and M.R. Somalu, Preparation of $SrFe_{0.5}Ti_{0.5}O_{3-\delta}$ perovskite-structured ceramic using the glycine-nitrate combustion technique, *Mater. Lett.*, 194(2017), p. 197.

[134] T.H.N.G. Amaraweera, D. Senarathna, and A. Wijayasinghe, Synthesis of Li $(Ni_{1/3}Mn_{1/3}Co_{1/3})O_2$ by Glycine Nitrate combustion process, *Ceylon J. Sci.*, 45(2016), No. 3, art. No. 21.

[135] T. Feng, B.B. Niu, J.C. Liu, and T.M. He, Sr- and Mo-deficiency $Sr_{1.95}TiMo_{1-x}O_{6-\delta}$ double perovskites as anodes for solid-oxide fuel cells using H_2S-containing syngas, *Int. J. Hydrogen Energy*, 45(2020), No. 43, p. 23444.

[136] H.H. Zhao, F.Y. Wang, L.R. Cui, X.Z. Xu, X.J. Han, and Y.C. Du, Composition optimization and microstructure design in MOFs-derived magnetic carbon-based microwave absorbers: A review, *Nano Micro Lett.*, 13(2021), No. 1, p. 1.

[137] S.A. Muhammed Ali, M. Anwar, M.R. Somalu, and A. Muchtar, Enhancement of the interfacial polarization resistance of $La_{0.6}Sr_{0.4}Co_{0.2}Fe_{0.8}O_{3-\delta}$ cathode by microwave-assisted combustion method, *Ceram. Int.*, 43(2017), No. 5, p. 4647.

[138] J.H. Xu, S.B. Wan, Y. Wang, *et al.*, Enhancing performance of molybdenum doped strontium ferrite electrode by surface modification through Ni infiltration, *Int. J. Hydrogen Energy*, 46(2021), No. 18, p. 10876.

[139] S. Vafaeenezhad, N. K. Sandhu, A. R. Hanifi, T. H. Etsell, and P. Sarkar, Development of proton conducting fuel cells using nickel metal support, *J. Power Sources*, 435(2019), art. No. 226763.

[140] P.P. Wu, Y.T. Tian, Z. Lü, X. Zhang, and L.L. Ding, Electrochemical performance of $La_{0.65}Sr_{0.35}MnO_3$ oxygen electrode with alternately infiltrated $Sm_{0.5}Sr_{0.5}CoO_{3-\delta}$ and $Sm_{0.2}Ce_{0.8}O_{1.9}$ nanoparticles for reversible solid oxide cells, *Int. J. Hydrogen Energy*, 47(2022), No. 2, p. 747.

[141] Q.M. Liu, S.Z. Huang, and A.J. He, Composite ceramics thermal barrier coatings of yttria stabilized zirconia for aero-engines, *J. Mater. Sci. Technol.*, 35(2019), No. 12, p. 2814.

[142] Y. Liu, X.Q. Han, Q. Huang, *et al.*, Structural damage response of lanthanum and yttrium aluminate crystals to nuclear collisions and electronic excitation: Threshold assessment of irradiation damage, *J. Mater. Sci. Technol.*, 90(2021), p. 95.

[143] T.Z. Wu, Y.Q. Zhao, R.R. Peng, and C.R. Xia, Nano-sized $Sm_{0.5}Sr_{0.5}CoO_{3-\delta}$ as the cathode for solid oxide fuel cells with proton-conducting electrolytes of $BaCe_{0.8}Sm_{0.2}O_{2.9}$, *Electrochim. Acta*, 54(2009), No. 21, p. 4888.

[144] S. Abdul, W. Yusoff, N. Baharuddin, M. Somalu, A. Muchtar, and N. Osman, Electrochemical performance of sol−gel derived $La_{0.6}S0.4CoO_{3-\delta}$ cathode material for proton-conducting fuel cell: A comparison between simple and advanced cell fabrication techniques, *Process. Appl. Ceram.*, 12(2018), No. 3, p. 277.

[145] L.M. Ding, L.X. Wang, D. Ding, S.H. Zhang, X.F. Ding, and G.L. Yuan, Promotion on electrochemical performance of a cation deficient $SrCo_{0.7}Nb_{0.1}Fe_{0.2}O_{3-\delta}$ perovskite cathode for intermediate-temperature solid oxide fuel cells, *J. Power Sources*, 354(2017), p. 26.

[146] X.J. Liu, D. Han, H. Wu, X. Meng, F.R. Zeng, and Z.L. Zhan, $Mn_{1.5}Co_{1.5}O_{4-\delta}$ infiltrated yttria stabilized zirconia composite cathodes for intermediate-temperature solid oxide fuel cells, *Int. J. Hydrogen Energy*, 38(2013), No. 36, p. 16563.

[147] F. Bidrawn, G. Kim, G. Corre, J.T.S. Irvine, J.M. Vohs, and R.J. Gorte, Efficient reduction of CO_2 in a solid oxide electrolyzer, *Electrochem. Solid State Lett.*, 11(2008), No. 9, p. 167.

[148] X.L. Yue and J.T.S. Irvine, Alternative cathode material for CO_2Reduction by high temperature solid oxide electrolysis cells, *J. Electrochem. Soc.*, 159(2012), No. 8, p. F442.

[149] Y.Q. Yu, L.X. Yu, K. Shao, *et al.*, $BaZr_{0.1}Co_{0.4}Fe_{0.4}Y_{0.1}O_3$-SDC composite as quasi-symmetrical electrode for proton conducting solid oxide fuel cells, *Ceram. Int.*, 46(2020), No. 8, p. 11811.

[150] J. Xu, X.L. Zhou, L. Pan, M.X. Wu, and K.N. Sun, Oxide composite of $La_{0.3}Sr_{0.7}Ti_{0.3}Fe_{0.7}O_{3-\delta}$ and CeO_2 as an active fuel electrode for reversible solid oxide cells, *J. Power Sources*, 371(2017), p. 1.

[151] M.K. Hossain, R. Chanda, A. El-Denglawey, *et al.*, Recent progress in Barium zirconate proton conductors for electrochemical hydrogen device applications: A review, *Ceram. Int.*, 47(2021), No. 17, p. 23725.

[152] H.F. Lv, L. Lin, X.M. Zhang, *et al.*, Promoting exsolution of RuFe alloy nanoparticles on $Sr_2Fe_{1.4}Ru_{0.1}Mo_{0.5}O_{6-\delta}$ via repeated redox manipulations for CO_2 electrolysis, *Nat. Commun.*, 12(2021), No. 1, art. No. 5665.

[153] G.S. Kim, B.Y. Lee, G. Accardo, H.C. Ham, J. Moon, and S.P. Yoon, Improved catalytic activity under internal reforming solid oxide fuel cell over new rhodium-doped perovskite catalyst, *J. Power Sources*, 423(2019), p. 305.

[154] R. Kannan, K. Singh, S. Gill, T. Fürstenhaupt, and V. Thangadurai, Chemically stable proton conducting doped $BaCeO_{3-\delta}$ -No more fear to SOFC wastes, *Sci. Rep.*, 3(2013), art. No. 2138.

[155] D.Q. Liu, Y.N. Dou, T. Xia, *et al.*, B-site La, Ce, and Pr-doped $Ba_{0.5}Sr_{0.5}Co_{0.7}Fe_{0.3}O_{3-\delta}$ perovskite cathodes for intermediate-temperature solid oxide fuel cells: Effectively promoted oxygen reduction activity and operating stability, *J. Power Sources*, 494(2021), art. No. 229778.

[156] W.N.A.W. Yusoff, N.A. Baharuddin, M.R. Somalu, A. Muchtar, and A.A. Samat, A short review on selection of electrodes materials for symmetrical solid oxide fuel cell, *IOP Conf. Ser.: Mater. Sci. Eng.*, 957(2020), No. 1, art. No. 012049.

[157] B. Hołówko, P. Błaszczak, M. Chlipała, *et al.*, Structural and catalytic properties of ceria layers doped with transition metals for SOFCs fueled by biogas, *Int. J. Hydrogen Energy*, 45(2020), No. 23, p. 12982.

[158] M.H. Shen and P.P. Zhang, Progress and challenges of cathode contact layer for solid oxide fuel cell, *Int. J. Hydrogen Energy*, 45(2020), No. 58, p. 33876.

[159] M. V. Sandoval, C. Cardenas, E. Capoen, P. Roussel, C. Pirovano, and G. H. Gauthier, Performance of $La_{0.5}Sr_{1.5}MnO_{4\pm\delta}$ Ruddlesden–Popper manganite as electrode material for symmetrical solid oxide fuel cells. Part B. the hydrogen oxidation reaction, *Electrochim. Acta*, 353(2020), art. No. 136494.

[160] S. Molin, J. Karczewski, B. Kamecki, A. Mroziński, S.F.

Wang, and P. Jasiński, Processing of $Ce_{0.8}Gd_{0.2}O_{2-\delta}$ barrier layers for solid oxide cells: The effect of preparation method and thickness on the interdiffusion and electrochemical performance, *J. Eur. Ceram. Soc.*, 40(2020), No. 15, p. 5626.

[161] D. Ramasamy, N. Nasani, D. Pukazhselvan, and D.P. Fagg, Increased performance by use of a mixed conducting buffer layer, terbia-doped ceria, for $Nd_2NiO_{4+\delta}$ SOFC/SOEC oxygen electrodes, *Int. J. Hydrogen Energy*, 44(2019), No. 59, p. 31466.

[162] X.Y. Chen, W.J. Ni, X.J. Du, *et al*., Electrochemical property of multi-layer anode supported solid oxide fuel cell fabricated through sequential tape-casting and co-firing, *J. Mater. Sci. Technol.*, 35(2019), No. 4, p. 695.

[163] W.N.A. Wan Yusoff, N.N.M. Tahir, N.A. Baharuddin, M.R. Somalu, A. Muchtar, and L.J. Wei, Effects of roller speed on the structural and electrochemical properties of $LiCo_{0.6}Sr_{0.4}O_2$ cathode for solid oxide fuel cell application, *Sustain. Energy Technol. Assess.*, 56(2023), art. No. 103096.

[164] P. Jasinski, S. Molin, M. Gazda, V. Petrovsky, and H.U. Anderson, Applications of spin coating of polymer precursor and slurry suspensions for solid oxide fuel cell fabrication, *J. Power Sources*, 194(2009), No. 1, p. 10.

[165] M. Chen, J.L. Luo, K.T. Chuang, and A.R. Sanger, Fabrication and electrochemical properties of cathode-supported solid oxide fuel cells via slurry spin coating, *Electrochim. Acta*, 63(2012), p. 277.

[166] E. Lay, L. Dessemond, and G. Gauthier, Ba-substituted LSCM anodes for solid oxide fuel cells, *J. Power Sources*, 221(2013), p. 149.

[167] M.K. Rath, B.G. Ahn, B.H. Choi, M.J. Ji, and K.T. Lee, Effects of manganese substitution at the B-site of lanthanum-rich strontium titanate anodes on fuel cell performance and catalytic activity, *Ceram. Int.*, 39(2013), No. 6, p. 6343.

[168] J.C. Ruiz-Morales, J. Canales-Vázquez, B. Ballesteros-Pérez, *et al*., LSCM-(YSZ-CGO) composites as improved symmetrical electrodes for solid oxide fuel cells, *J. Eur. Ceram. Soc.*, 27(2007), No. 13-15, p. 4223.

[169] J. Lu, Y.M. Yin, J.C. Li, L. Xu, and Z.F. Ma, A cobalt-free electrode material $La_{0.5}Sr_{0.5}Fe_{0.8}Cu_{0.2}O_{3-\delta}$ for symmetrical solid oxide fuel cells, *Electrochem. Commun.*, 61(2015), p. 18.

[170] Y.F. Tian, W.J. Wang, Y. Liu, *et al*., Cobalt-free perovskite oxide $La_{0.6}Sr_{0.4}Fe_{0.8}Ni_{0.2}O_{3-\delta}$ as active and robust oxygen electrode for reversible solid oxide cells, *ACS Appl. Energy Mater.*, 2(2019), No. 5, p. 3297.

[171] M.V. Sandoval, S. Durán, A. Prada, *et al*., Synthesis and preliminary study of $Nd_xAE_{2-x}MnO_{4\pm\delta}$ (AE: Ca, Sr) for symmetrical SOFC electrodes, *Solid State Ion.*, 317(2018), p. 194.

[172] T.L. Zhu, D.E. Fowler, K.R. Poeppelmeier, M.F. Han, and S.A. Barnett, Hydrogen oxidation mechanisms on perovskite solid oxide fuel cell anodes, *J. Electrochem. Soc.*, 163(2016), No. 8, p. F952.

[173] C.H. Yang, Z.B. Yang, C. Jin, G.L. Xiao, F.L. Chen, and M.F. Han, Sulfur-tolerant redox-reversible anode material for direct hydrocarbon solid oxide fuel cells, *Adv. Mater.*, 24(2012), No. 11, p. 1439.

[174] T.H. Shin, Y. Okamoto, S. Ida, and T. Ishihara, Self-recovery of Pd nanoparticles that were dispersed over $La(Sr)Fe(Mn)O_3$ for intelligent oxide anodes of solid-oxide fuel cells, *Chem. Eur. J.*, 18(2012), No. 37, p. 11695.

[175] Y.M. Xu, Z.H. Lin, W. Wei, *et al.*, Recent progress of electrode materials for flexible perovskite solar cells, *Nano Micro Lett*., 14(2022), art. No. 117

[176] X.Y. Luo, Y. Yang, Y. Yang, *et al*., Reduced-temperature redox-stable LSM as a novel symmetrical electrode material for SOFCs, *Electrochim. Acta*, 260(2018), p. 121.

[177] W. He, J.C. Fan, H. Zhang, M.N. Chen, Z.M. Sun, and M. Ni, Zr doped $BaFeO_{3-\delta}$ as a robust electrode for symmetrical solid oxide fuel cells, *Int. J. Hydrogen Energy*, 44(2019), No. 60, p. 32164.

[178] S. Wang, B. Wei, and Z. Lü, Electrochemical performance and distribution of relaxation times analysis of tungsten stabilized $La_{0.5}Sr_{0.5}Fe_{0.9}W_{0.1}O_{3-\delta}$ electrode for symmetric solid oxide fuel cells, *Int. J. Hydrogen Energy*, 46(2021), No. 58, p. 30101.

[179] M. Bilal, J. Gao, K. Shaheen, *et al*., Performance evaluation of highly active and novel $La_{0.7}Sr_{0.3}Ti_{0.1}Fe_{0.6}Ni_{0.3}O_{3-\delta}$ material both as cathode and anode for intermediate-temperature symmetrical solid oxide fuel cell, *J. Power Sources*, 472(2020), p. 228498.

[180] H.L. Tao, J.J. Xie, Y.F. Wu, and S.R. Wang, Evaluation of $PrNi_{0.4}Fe_{0.6}O_{3-\delta}$ as a symmetrical SOFC electrode material, *Int. J. Hydrogen Energy*, 43(2018), No. 32, p. 15423.

[181] B. Admasu Beshiwork, B. Sirak Teketel, X.Y. Luo, *et al*., Nanoengineering electrode for yttria-stabilized zirconia-based symmetrical solid oxide fuel cells to achieve superior output performance, *Sep. Purif. Technol.*, 295(2022), art. No. 121174.

[182] Y.H. Gu, Y.L. Zhang, Y.F. Zheng, H. Chen, L. Ge, and L.C. Guo, $PrBaMn_2O_{5+\delta}$ with praseodymium oxide nano-catalyst as electrode for symmetrical solid oxide fuel cells, *Appl. Catal., B*, 257(2019), p. 117868.